Physics – Uspekhi **45** (10) 1051 – 1072 (2002)

REVIEWS OF TOPICAL PROBLEMS PACS numbers: **05.65.+b**, 75.60.Eg, 75.60.Ch, 75.70.Kw

New phenomena in the low-frequency dynamics of magnetic domain ensembles

G S Kandaurova

DOI: 10.1070/PU2002v045n10ABEH001064

Contents

Abstract. Research into the phenomenon of dynamic self-organization and the excited ('anger') state of multidomain magnetic films with perpendicular anisotropy is reviewed. The phenomenon was discovered in 1988 when studying the domain structure of iron garnet films in low-frequency (0.1–10 kHz) ac magnetic fields.

1. Introduction

The magnetic properties of soft magnetic materials are largely determined by the behavior of the domain structure of the material in ac magnetic fields of moderate frequencies (0.1 – 10 kHz) [1]. The method and geometry of experiments in visualizing magnetic domains in such materials make it possible to observe only surface domains. Only indirect data provide information about the shape and size of domains in the bulk of samples (domain wall bending, penetrating and nonpenetrating domains, etc.). More than that, the ensemble of domains that can be monitored is usually not very large. At the same time, cooperative effects related to the behavior of the entire domain structure of the sample as a whole in magnetization and magnetization reversal may play an important role in forming the technologically important properties of these materials [1]. When studying the behavior of a large ensemble of interacting domains in an ac magnetic field, it is most advisable to select magnetically uniaxial films as the objects of investigation, films in which the easy axis (EA) is perpendicular to the film surface. In such films (thin layers), there is what is known as a labyrinth domain structure (Fig. 1a, upper part), described in theory by the well-known model of plane-parallel penetrating domains, or the Kittel model. In our experiments, we studied optically transparent epitaxial (111) iron garnet (IG) films with perpendicular anisotropy and an initial domain structure as in Fig. 1a, with the characteristic size of the structure, i.e., the width (period) of the stripe domains in the labyrinthine structure, being two to three orders of magnitude smaller than the sample size in the plane.

The domain structure of IG films was intensely studied in the 1970s and 1980s in view of the prospect of using such films in memory devices of microelectronics to record information in magnetic domains and domain walls and also in devices of magnetically controlled optics [2, 3]. The domain structure (DS) in static magnetic fields has been studied fairly thoroughly, both theoretically and experimentally. As for the dynamics, attention has been focused primarily on the analysis of nanosecond magnetization-reversal processes (e.g., the formation of the reversed magnetic phase [3]) and on the study of properties of individual magnetic bubbles and domain walls (including the elements of their internal structure) in ac (pulsed, local) magnetic fields with frequencies to 10 – 100 MHz or higher. Such a range was determined by the requirement of high speed of operation of the above-noted devices.

The frequency range from 0.1 to 10 kHz proved to be ignored. The experiments discussed in Refs [4 – 8] used IG films with an initial penetrating labyrinthine structure placed in a spatially uniform, continuously operating low-frequency

G S Kandaurova A M Gor'kiĭ Ural State University
ul. Lenina 31, 620083 Ekaterinburg, Russian Federation
Tel. (+7-3432) 61 68 23. Fax (+7-3432) 61 59 78
E-mail: gerta.kandaurova@usu.ru

Received 12 July 2001, revised 25 December 2001
Uspekhi Fizicheskikh Nauk **172** (10) 1165 – 1187 (2002)
Translated by E Yankovsky; edited by S N Gorin

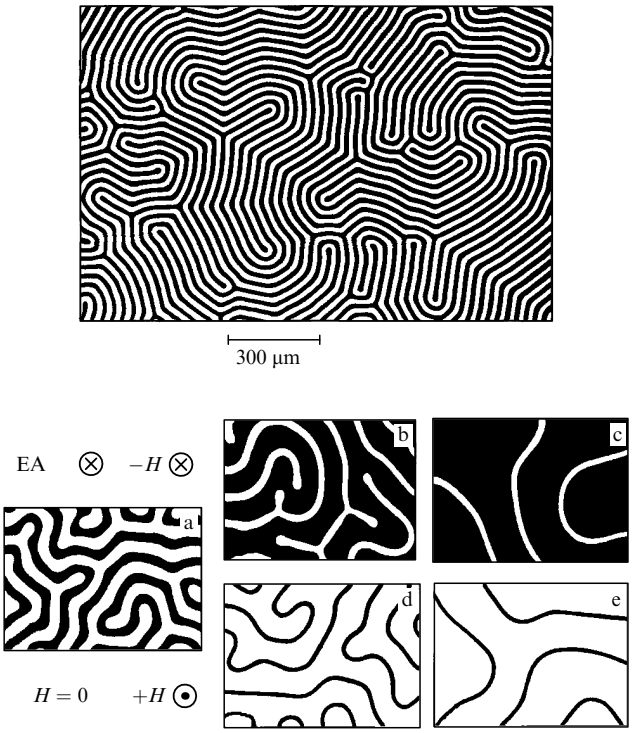

Figure 1. Typical patterns of the labyrinth domain structure of films with perpendicular anisotropy in a zero magnetic field (the upper part of the figure and a) and in a gradually increasing magnetic field of one (b and c) and the opposite (d and e) directions. The magnetization vectors $\mathbf{J}_s$ are directed 'toward us' and 'away from us'.

oscillating magnetic field. They revealed the presence of an entirely new excited state of a multidomain magnetic medium, which we called [8] an 'anger' state (AS). The most characteristic feature of 'anger' states is the self-organization of a disordered (we call it chaotic) ensemble of interacting domains and the formation of ordered stable dynamic domain structures (DDSs) of various types. Among these, ring and spiral dynamic domains proved to be the most common. Thus, it was shown for the first time that multidomain magnetic media are objects of synergetics [9].

In our studies of this phenomenon we discovered a whole new range of effects and laws. The topic of the present review is a description of these effects and laws. Note that after our first publications on the topic [4–8], research began in such areas as the study of different types of dynamic self-organization in ensembles of magnetic domains, the experimental and theoretical study of the properties of static and dynamic spiral and ring domains, and the analysis of the various features of the dynamics of a system of magnetic domains (e.g., see Refs [10–20]). I, however, did not attempt to present a full review of research on the dynamics of magnetic domains; the scope of the review is limited to the results of original research in the 'anger' state and DDSs in a continuously operating ac magnetic field.

2. Experimental

The basic objects of our research into the behavior of the domain structure in ac magnetic fields were mainly epitaxial (single-crystal) iron garnet (IG) films with the (111) plane. In the demagnetized state, $R_3(FeGa)_5O_{12}$ films, where $R = (YBi)$, (LuBi), (TmBi), or (YLuBi), exhibit induced perpendicular uniaxial anisotropy and a single-type labyrinth structure (Fig. 1a).

In Figure 1 the magnetization vectors $\mathbf{J}_s$ in the light and dark stripe domains are directed along the normal to the film 'toward us' and 'away from us,' respectively. The values of the characteristic parameters of the film sample under investigation were spread over fairly broad intervals: the diameter of the samples was approximately 4–5 mm; the film thickness $L = 4.5–40$ μm; the width d_0 of the domains in the demagnetized state and the domain structure period $P_0 = 2d_0 = 4–41$ μm; the saturation magnetization $J_s = 6.5–32$ G; the anisotropy field $H_a = 2K/J_s$, where K is the constant of induced uniaxial perpendicular anisotropy, was 1.3–13 kOe, the Q factor $Q = K/(2\pi J_s^2)$ was 3–96; and the saturation field along EA $H_s = 30–190$ Oe. The coercive force of the samples, related to the time lag in the displacement of the domain walls, did not exceed 1.5 Oe. (For more details on the sample parameters, see Section 9.)

The method of visual observation of both static and dynamic domains was based on the magnetooptic Faraday effect. The photographic exposure was 0.4–1 ms. A spatially uniform dc bias field (H_b) or an ac magnetic field of the 'alternating-sign symmetric meander' type (H_Π) or a 'harmonic field' $H_\sim = H_0 \sin(2\pi ft)$ with a frequency $f = 0.1–150$ kHz and an amplitude H_0 up to 200 Oe was directed along the normal to the sample, i.e., along the EA. Thus, in the case of an ac field, the films were continuously pumped. We also note that all experiments were conducted in roughly the same way: a demagnetized state with a single-type labyrinthine domain structure (Fig. 1a) was created via magnetic 'shaking' in an ac field with a frequency $f = 50$ Hz and an amplitude that decreased from $H_0 \leqslant H_s$ to zero; after that, the frequency f of $H_\sim$ or H_Π was fixed and the amplitude H_0 of the ac field was gradually increased. The exposure to each measured value of H_0 was no less than 20 s. The temperature was kept constant throughout the entire experiment. This experimental scheme made it possible to reduce the effects of magnetic history of the samples to a minimum and to achieve the best reproducibility of the experimental results.

3. Dynamic self-organization. Ring and spiral dynamic domains

As noted earlier, the domain structure of the samples in the initial state (Fig. 1) is disordered (of the labyrinth type). It remains such under magnetization in a dc field (Figs 1a–1e). If the properties of the film in its plane are entirely isotropic, then under multiple repetition of the process of quasi-static magnetization in the field of one (Figs 1b and 1c) or the opposite (Figs 1d and 1e) directions the DS patterns are not reproduced, domain walls are in different places, the stripe domains are bent differently. The reason is that, due to the interaction with microdefects and other domains, a domain wall moves in jumps and for each small section of the domain wall this motion is of a probabilistic nature. Here, however, the average width d_1 of the domains magnetized along the field (this is the main magnetic phase with $\mathbf{J}_s \uparrow\uparrow \mathbf{H}$), the average width d_2 of the domains magnetized against the field (the reverse magnetic phase with $\mathbf{J}_s \uparrow\downarrow \mathbf{H}$) and the average period $P = d_1 + d_2$ depend on the strength of the external field in a definite manner. If the coercive force of the sample is small, the theory provides a good description of this dependence [21].

In an ac field, the domain wall motion is disordered (chaotic), and the disorder increases with the frequency f and amplitude H_0 of the field. The domain structure observed in a microscope becomes completely smeared. However, beginning with certain values of f and H_0, the state of the ensemble of moving domains changes dramatically: as a result of self-organization, there emerge sharp, contrast, and easily observable (which means stable) DDSs with a definite geometry. The random motion of domain walls transforms into oscillatory motion about relatively stable positions of equilibrium.

As an example, we give the experimental data for two IG films whose parameters are listed in the captions to Figs 2 and 3. The films differed in their Q factors by an order of magnitude. In the first film (Fig. 2) with a fairly moderate value $Q = 9$, in an ac field of the meander type H_Π within narrow frequency and amplitude intervals ($f = 0.1-0.2$ kHz), ordered DDSs shaped as ring domains (RD) or systems of concentric ring domains (CRDs) are formed similar to the system depicted in Fig. 2a. Within a much broader frequency interval $f = 0.2-6$ kHz (Figs 2b and 2c), dynamic spiral domains (SD) are formed. Note that in the given sample, no ordered DDSs are formed in a harmonic ac field.

By contrast, in the second, highly anisotropic film ($Q = 96$), the processes of dynamic self-organization manifested themselves most vividly in a harmonic field $H_\sim = H_0 \sin(2\pi ft)$. Beginning with the minimum frequency $f_b \approx 1.5$ kHz and up to 6 kHz, large, stable, and beautifully

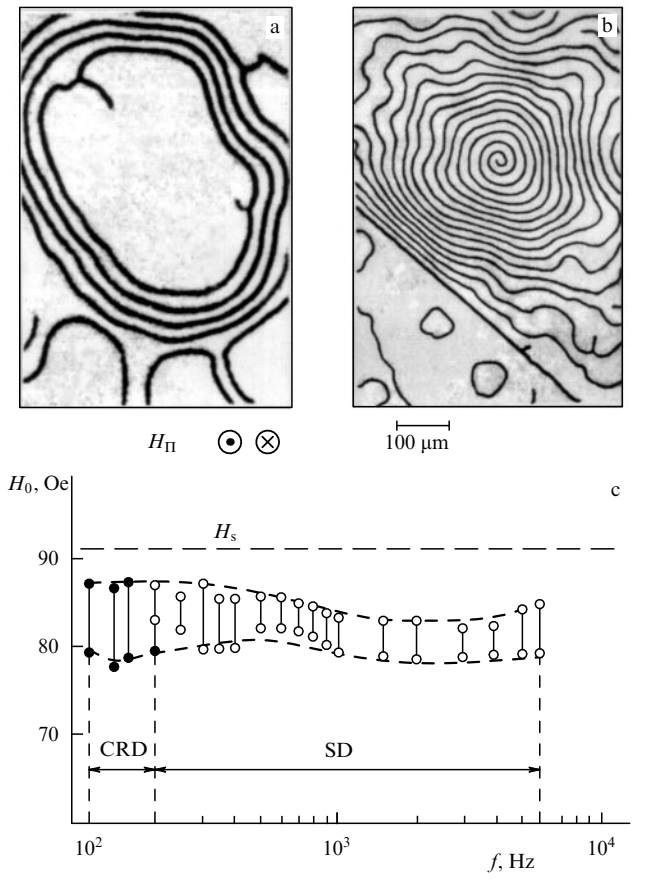

Figure 2. (a) Dynamic concentric ring domains, (b) spiral domains, and (c) the amplitude–frequency region of their existence in an $(YSm)_3(FeGa)_5O_{12}$ film with $L = 5$ μm, $P_0 = 11$ μm, and $Q = 9$.

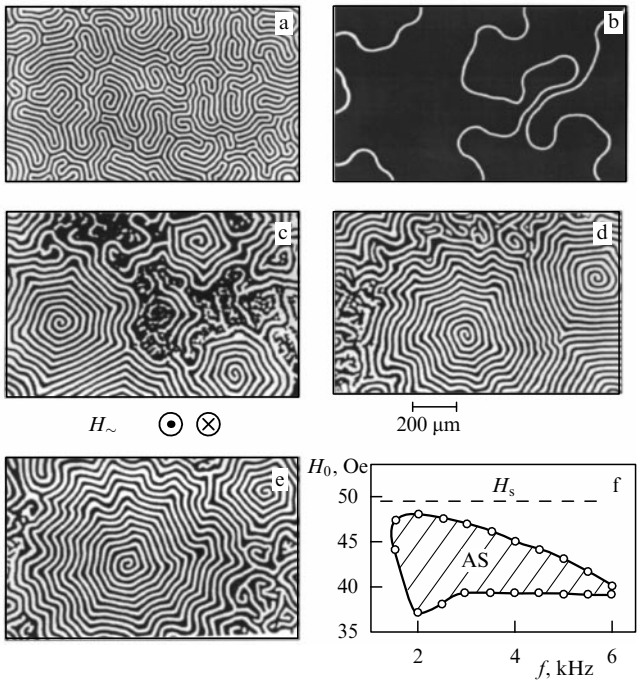

Figure 3. Domain structure of the iron garnet film $(YLuBi)_3(FeGa)_5O_{12}$ with $L = 9.5$ μm, $P_0 = 33$ μm, and $Q = 96$ (a) in the initial demagnetized state, (b) in a constant-bias field $H_b = 43$ Oe, (c, d, and e) in a harmonic field $H_\sim$ with an amplitude $H_0 = 43$ Oe and frequency $f = 3$ kHz, (f) the anger state (AS) region. The micrographs in figures c, d, and e were taken with a time lag of 20–30 s.

shaped multiturn SDs (Figs 3c–3e) arise. The stripe domains in the SD turns are 'broken' in such a way that the spiral is of a sectorial nature. Presumably, this feature results from the weak manifestation of the natural magnetocrystalline anisotropy of the IG film. In the cubic lattice of the IG film, the four ⟨111⟩ axes are EAs. One of these, [111], coincides with the EA of the induced uniaxial anisotropy of the film, while the other three are tilted with respect to the (111) plane at an angle of approximately 20°. Their projections onto the (111) plane are oriented at an angle of 60° with respect to each other. Hence, one could expect a preferred alignment of the stripe domains in the turns of the dynamic SDs along these directions and, respectively, the existence of six sectors in the SD pattern in Fig. 3, i.e., the SD should have a hexagonal shape. However, the broken nature of the turns in the SDs in Fig. 3 is more complicated. One cannot rule out the possibility that all this is a manifestation of the effect of domain wall reorientation in a magnetic field in IG crystals with combined anisotropy. Note that in the film in question no CRD systems similar to those shown in Fig. 2a are formed. It must also be acknowledged that today we have no convincing explanation of such different behavior of the two IG thin-film samples described here.

Compared to dynamic SDs, the dynamic CRD systems that are formed at low frequencies (100–200 Hz) have been observed by us rather infrequently. Hence, the geometric and dynamic properties of this type of CRD have been poorly studied. A characteristic feature of CRD systems noted in Refs [5, 6, 8] is the fact that they consist of a small number of rings (two to five rings of domains of the same polarity). The period of the structure in a CRD is approximately two to three times larger than P_0, the DS period in a zero field. At the same time, the diameter of the inner ring exceeds P_0 by 1 to

1.5 orders of magnitude. It has been noted that a DDS consisting of several interacting CRD systems forming a network is more stable.

Static ring domains have been studied somewhat more thoroughly by other researchers. Such domains are formed when, in the presence of a dc bias field H_b, a series of pulses of magnetic field, H_p, is applied to the IG film. Logunov and Moiseev [22, 23] have detected (for different pulse lengths) in the (H_p, H_b) plane the presence of limited regions of CRD formation. It was shown that the region of existence of CRDs in H_p is the widest near the value of H_B corresponding to the elliptic instability of magnetic bubbles. It has also been found that there is a certain relationship between CRD formation and the presence of microdefects in the film. Lamonova et al. [24] observed in a static magnetic field the presence of ring domains surrounded by a lattice of magnetic bubbles. A theoretical model for a system of static CRDs has been proposed. The total energy of such a domain configuration and its dependence on the various characteristics of the magnetic material (film), the geometric parameters of the CRD system, and the strength of the external static magnetic field have been calculated. It has been found that an equilibrium CRD system may exist only if the number of rings is small. (We will return to the problem of ring domains in Section 5, where we will discuss dynamic domain structures of the leading-center type.)

Experiments have shown that SD formation starts at a certain minimum threshold frequency f_b and occurs only within a limited range of amplitudes and frequencies of the ac field (Figs 2c and 3f). When the values of H_0 and f are within this region, dynamic SDs surrounded by a chaotic DDS are formed, while outside this (H_0–f) region only chaotic dynamic domain structures are observed. The shape, size, and arrangement in the (H_0–f) regions of dynamic order are different for different samples (cf. Figs 2c and 3f) and strongly depend on temperature [7, 8, 11] and the shape of the ac field, i.e., the function $H(t)$. For instance, there are films in which self-organization, or SD formation, occurs in a field of a meander type (H_Π) but does not occur in a harmonic field ($H_\sim$), while in other films the situation is just the opposite [5, 6, 8]. Finally, there are films in which self-organization occurs in ac fields of both types but in different ranges of H_0 and f.

The dynamic domains in different samples (cf. Figs 2–5) can have very different shapes, e.g., weakly and strongly distorted spirals, with a small or large core, with a few or many turns, isolated and coupled spiral domains, close-packed structures of spirals, one- and two-arm SD structures with the same or different twist directions, etc. Figure 4 depicts a fragment of a very large SD resembling the spiral of Archimedes. The SD pattern is triple-contrast: there are white, black, and gray stripe domains in the turns of the spiral, In all domains, the $\mathbf{J}_s$ vectors are directed either 'toward us' or 'from us.' In the white and black domains this orientation does not change during exposition while photographing the SD, while in the gray parts the orientation changes due to the vibration of domain walls that is caused by cyclic variation of the field (for more detail, see Ref. [8]).

Observations have revealed that in the same sample the configuration of the dynamic SDs and their geometric parameters (the maximum SD diameter, the number of turns, the diameter of the core, the distance between the turns in the central part and on the periphery) may strongly depend on the field frequency and amplitude [7, 25]. For instance, Figs 5a–5c show the SDs in the same area of the sample of the films under investigation for different values of H_0 and f of the field $H = H_0 \sin(2\pi ft)$. Clearly, these SDs differ dramatically, with the size of the SD core rapidly decreasing with growing frequency (Fig. 5d). We do not possess the full information about the dependence of the size of the SD core on the field frequency for other IG films. Nevertheless, we would like to mention certain experimental facts. As Fig. 2c shows, at low frequencies ($f = 100$–200 Hz) the inner ring of the CRD systems that are formed (Fig. 2a)

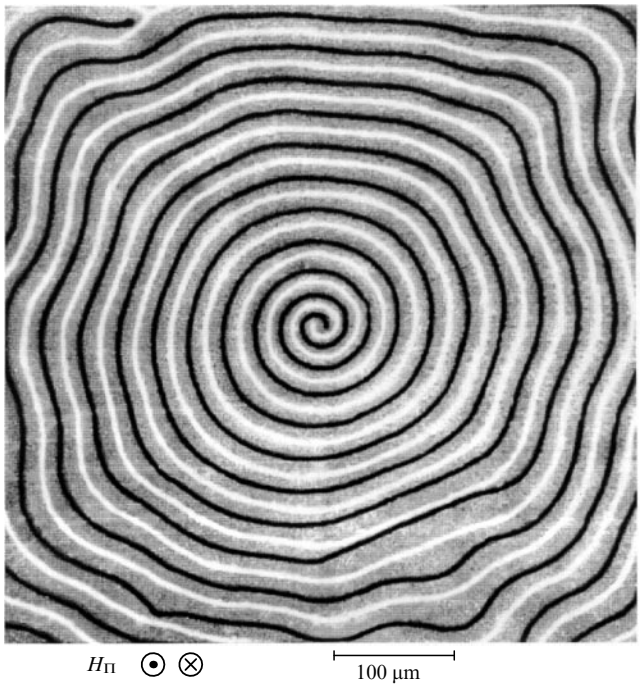

Figure 4. Multiturn dynamic SD in the $(YSm)_3(FeGa)_5O_{12}$ film with $L = 10$ μm, $P_0 = 25$ μm, and $Q = 20$ in a meander-type field H_Π with an amplitude of 40 Oe and a frequency of 300 Hz.

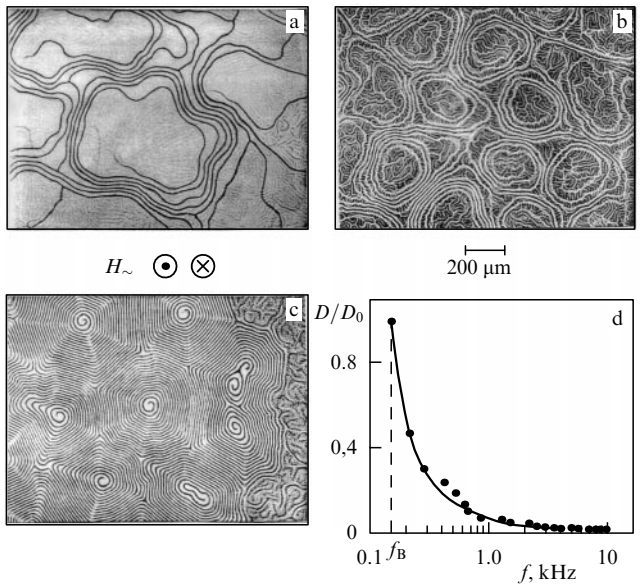

Figure 5. Dynamic SDs in a $(TmBi)_3(FeGa)_5O_{12}$ film with $L = 6$ μm, $P_0 = 17$ μm, and $Q = 21$ in a field $H_\sim$ with an amplitude equal to (a) 51.1, (b) 52.4, and (c) 44.9 Oe and a frequency equal to 0.15, 0.50, and 5 kHz, respectively, and (d) the frequency dependence of the relative diameter of the SD core.

has a very large diameter, more than 500 μm. Beginning with 300 Hz, dynamic SDs with a core size of roughly 10 μm are formed. The transition from one DDS type to another occurs in the range of 200–250 Hz. Here, in addition to CRD systems, spiral domains with a core as large as hundreds of microns may form. Within a large SD core or inside the CRD system, in each half-period of the field, a disordered DDS grows or disappears. This also happens with the other sample (Fig. 3). In it, at frequencies $f \geqslant 1500$ Hz, large multiturn SDs with small cores are formed (Figs 3c–3e). Actually (see Fig. 10 in Section 7), SDs emerge already at $f \approx 200-300$ Hz, and these are large SDs with a large core but with a small number of turns, which at higher frequencies transform into such SDs as are depicted in Figs 3c–3e. Thus, the rapid decrease of the diameter of the SD core as the frequency of the alternating field increases is, probably, a general law, which manifests itself in different IG films to a different degree.

In almost all samples of iron garnet films, we observed, for both $H_{\sim}$ and H_{Π}, DDS refinement (fragmentation) and the formation of a close-packed lattice of dynamic SDs as the field frequency increased [7, 8, 25]. A qualitative explanation of the fragmentation effect is given in Ref. [25], where a very simple theoretical model is used. The idea on which this model is based is that in low-frequency ac fields (in which case we can ignore the internal dynamic transformations of domain walls [2]), such a domain structure is energy-advantageous in which the domain walls rapidly relax to equilibrium. The possible reasons for the differences in the relaxation times of the stripe, labyrinthine, and spiral DSs have been discussed in Ref. [25]. For an ac field of the symmetric meander type, H_{Π}, an approximate expression for the quasi-equilibrium domain width (or the structure period P) was derived within the model of a stripe domain structure [21] at the end of a field pulse:

$$P = P_{0H} - \frac{J_e L f H}{2aV}\,, \tag{3.1}$$

where P_{0H} is the equilibrium DS period in a dc field H equal in magnitude to the amplitude value H_0 of the ac field, V is the domain-wall velocity, and a is a frequency-independent constant. Clearly, the period P of a dynamic DS is smaller than the period of a static DS under comparable conditions.

It must be noted that this effect of dynamic DS fragmentation has also been observed by other researchers [1, 27–29], who used other materials and other geometries of the experiments and interpreted the results differently. As for the formation of a close-packed system of multiturn SDs similar to that depicted in Fig. 5c, observations of such a static structure in thin magnetouniaxial single-crystal MnAlGe plates of the basal orientation in a demagnetized state were first reported in Ref. [30]. There, one can find a micrograph of a labyrinthine domain structure in the form of a square lattice consisting of one- and two-arm multiturn spiral domains and an interpretation of these domains. In Ref. [30], it was assumed that the alignment of sections of the stripe domains in the spirals is caused by the block nature (mosaicity) of the tetragonal single crystal and, respectively, the anisotropic distribution of the internal stresses of opposite signs. The pertinent diagram can also be found in Ref. [30].

Chetkin et al. [31] observed a close-packed system of SDs in iron garnet films. The hexagonal SD lattice has been studied both experimentally and theoretically [32, 33]. Spiral domains were observed after the samples were subjected to pulsed magnetic fields in combination with a dc bias field H_B, and the dependence of the energy density of a lattice of identical SDs of hexagonal shape on the geometric SD parameters was calculated.

In discussing the various works that deal with the observation and study of separate SDs in zero or quasi-static fields there is a need to maintain a certain chronological order.

In their study of the magnetic hysteresis and domain structure of the highly anisotropic magnetouniaxial alloy MnBi, Shur et al. [34] observed spiral domains on a thin ($L \sim 1$ μm) single-crystal film small in the basal plane (~ 15 μm). Each spiral domain repeated the hexagonal natural faceting of the miniature crystal. A theoretical model of such a domain structure in a simplified version was proposed and developed by Solov'ev and Onoprienko [35].

SD formation in an IG film was recorded by Hanna et al. [36]. When the strength of the dc bias field was reduced starting from the saturation value and, at the same time, a weak ac field was maintained, a domain shaped as a hexagonal spiral formed in a (111) film. The researchers believed that such a shape can be explained by the fact that magnetocrystalline anisotropy with the EAs parallel to ⟨111⟩ becomes noticeable against the background of induced uniaxial perpendicular anisotropy.

The gradual twisting of a stripe domain growing out of a local defect to form a multiturn spiral as the field strength decreases has been studied by Logunov and Randoshkin [37]. The shape of the SDs was similar to that of the spiral of Archimedes. The researchers suggested using IG films with such a domain structure as a magnetooptic deflector–concentrator [38].

Many researchers studied, both experimentally and theoretically, the formation and stability of a single static SD, the effect of temperature, magnetic field, and the surrounding domain structure, as well as of defects and other factors on the parameters of such a domain [13, 15–19, 39–42].

The above works deal with studies of RDs and SDs in static and low-frequency spatially uniform ac magnetic fields. Here, we do not mention the important work done in the field of dynamic RDs and SDs that are generated by a strong local pulse of a microwave field applied to an iron garnet film magnetized to saturation (e.g., see Refs [2, 3] and a thorough review in Ref. [43]).

Several researchers [13, 15, 17, 18, 32] connect the formation of spiral domains and their stability in dc fields with a magnetostatic interaction between the stripe domains in the turns of a spiral domain and between the SD and the surrounding domain structure. The latter interaction is taken into account on the basis of the idea of magnetostatic pressure [44] of different neighboring domain magnetic phases (a lattice of stripe domains or magnetic cylindrical domains (CDs), a honeycomb DS). Other researchers [37, 38, 45, 46], when dealing with the mechanism by which a stripe domain is twisted into a spiral, assign the leading role to the gyrotropic force $\mathbf{F}_g$ that acts on the head of the growing stripe (or dumbbell-shaped) domain and twists it. If we assume, as an approximation, that $\mathbf{F}_g$ is similar to the gyrotropic force acting on a CD during the bubble motion in a gradient magnetic field, then, according to Ref. [2],

$$\mathbf{F}_g = 4\pi J_s \gamma_{\text{eff}}^{-1} LS[\mathbf{z}_0 \times \mathbf{V}]\,, \tag{3.2}$$

where γ_{eff} is the effective gyromagnetic ratio of a multisublattice IG, L is the thickness of the film, z_0 is the unit

vector specifying the orientation of the magnetization outside the domain, and S is a parameter related to the internal structure of a domain wall. The magnitude and sign of S strongly depend on the type and number of Bloch lines in the wall. Various researchers [11, 45–48] point out the important role that Bloch lines play in the formation of SDs. The sign of S determines the direction of twist of a stripe domain (clockwise or counterclockwise) or, in other words, the topological charge of an SD ($+q$ or $-q$).

Nikolaev et al. [48] used high-speed photography to observe such transformations in the wall of an SD in the course of a magnetic-field pulse (the pulse length was 7 μs) that served as indications of generation and existence of many vertical Bloch lines. We cannot rule out the possibility that in a low-frequency oscillating field there is generation and buildup of Bloch lines, e.g., as the domain wall travels many times through local microdefects. The factors that could impede the formation of dynamic SDs are flexural instability of a stripe domain [49] and the high density of domains in the domain ensemble surrounding an SD.

Experiments have shown [8, 25] that the combination of an ac magnetic field and a low dc magnetizing (bias) field $H_b < H_s$ may strongly alter the geometry and properties of dynamic SDs. Here are some experimental facts that serve as indications of such a situation.

(1) The introduction of H_b lifts the degeneracy with respect to the direction of twist of the stripe domains in dynamic SDs, i.e., to the sign of the topological charge, $+q$ and $-q$. One of these becomes preferred. (Such a situation was observed by Lisovskiĭ and Mansvetova [45] in the SDs preserved after the ac field was switched off.) The reason is the breaking of symmetry in the amplitude values of the ac field ($H_0^+ = H_0 + H_b$ and $H_0^- = H_0 - H_b$) and, respectively, the difference in the conditions under which the dynamic SDs are formed. As H_b increases, the number of spirals with, say, $+q$ increases, while the number of spirals with $-q$ decreases up to the point where all SDs with such a twist disappear. In another sample, the situation may be just the opposite, i.e., for a given H_b the SDs with $-q$ are predominant. According to Loginov et al. [50], this experimental fact can be explained by the opposite sign of the effective gyromagnetic ratio γ_{eff} and hence [according to Eqn (3.2)] by the opposite direction of $\mathbf{F}_g$, all other things being equal.

(2) As H_b increases and as the upper boundary of the region of existence of dynamic SDs (Figs 2c and 3f) is approached (with $f = \text{const}$), in some films one can observe a sharp decrease of the number of turns in the SDs, formation of double- and single-turn SDs, and the disappearance of SDs. Other samples may not exhibit such behavior, and transition from the region of dynamic order is done in another way (see Section 4).

(3) Part of dynamic SDs with a small number of turns transform, just before they disappear, into a state of very rapid rotation, which can easily be observed. We called this state the (spinning) 'top' state [8]. Presumably, this state is related to the accumulation of Bloch lines as the length of the turns of a spiral domain decreases and the stored energy partially dissipates via the kinetic channel.

Today, there is no theory of dynamic spiral (and ring) domains. Using the approximation of small-amplitude modulation of magnetization, Borisov et al. [10] showed that spiral magnetization waves, or spiral solitons, may exist (at least in theory) in films with perpendicular anisotropy. In our first work [5], we also assumed that SDs are formations of soliton type. However, judging from the magnetooptic contrast of the observed spiral patterns, here we are dealing with domains. The $\mathbf{J}_s$ vectors in adjacent dynamic domains are antiparallel, as they are in static domains (Figs 1 and 3). Not a single one of the above patterns of behavior has a convincing theoretical justification. In some particular cases, only very general qualitative ideas and highly approximate models can be formulated.

4. The 'anger' state of a multidomain magnetic medium

Along with self-organization and chaos ⇒ order transitions in the amplitude – frequency ($H_0 - f$) region specified in Figs 2 and 3, there are also inverse processes in the domain system, i.e., order ⇒ chaos transitions. We were the first to point out in Refs [5, 8] that each generated spiral domain 'lives' a certain time T_g (the lifetime) and then disappears. This lifetime T_g is several orders of magnitude longer than the period of the ac magnetic field. A new spiral domain or several new domains appear within the monitored region after a certain time T_w (the wait time). A comparison of the frames in Figs 3c – 3e and 6a – 6c clearly shows a renovation of the picture of spiral domains in the course of one to two minutes. For instance (Fig. 6a), at a certain moment, within the observed section of the film a large multiturn spiral with a counterclockwise twist ($-q$) appears. After the life of this SD has expired and time T_w has elapsed, two spirals with equal topological charges ($-q$) emerge in the same place (Fig. 6b). After they have disappeared and time T_w has elapsed, two other spirals with

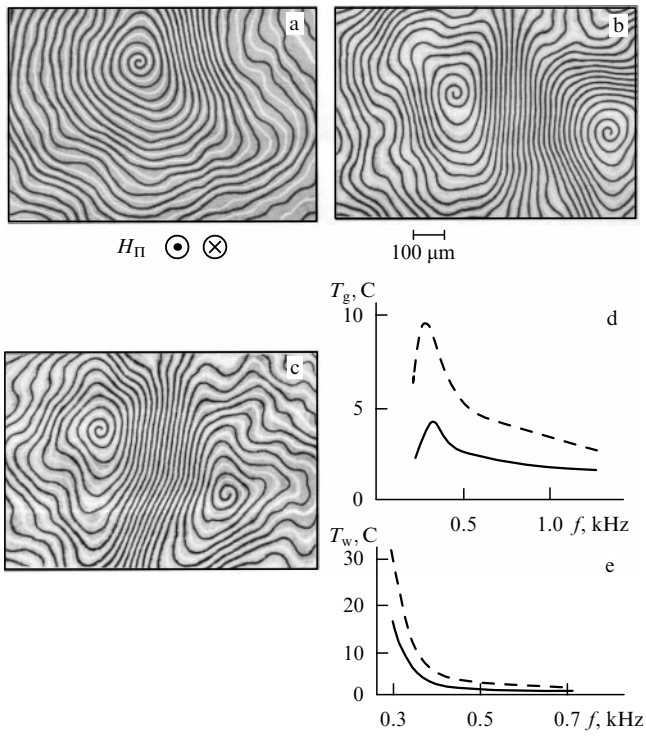

Figure 6. (a, b, and c) Dynamic spiral domains in the iron garnet film $(YSm)_3(FeGa)_5O_{12}$ with $L = 5$ μm, $P_0 = 11$ μm, and $Q = 9$ in an ac magnetic field of the meander type of frequency $f = 300$ Hz and amplitude $H_0 = 80$ Oe photographed at the same place of the sample within intervals shorter than one minute. The frequency dependence of (d) the lifetime and (e) the wait time for the emergence of a spiral domain.

$+q$ and $-q$ appear (Fig. 6c). This process continues on the average with a frequency $f_s = 1/(T_g + T_w)$. For the given film at $f = 350$ Hz and $H_0 = 82$ Oe, the maximum values of T_g and T_w may be approximately 10 s and 30 s, respectively. Ring DDSs behave similarly in their $(H_0 - f)$ region [5, 8]. Chaos $\Leftrightarrow$ order transitions continue as long as the ac magnetic field is switched on and the appropriate experimental conditions are maintained.

An iron garnet film placed in a constantly operating spatially uniform ac magnetic field constitutes an open thermodynamic system in which there is influx and dissipation of energy combined with *self-organization* of the system's elements (domains). This makes it possible to classify multidomain iron garnet films as active media examined, in particular, in synergetics (e.g., see Ref. [9]). The following important points should be stressed here. The well-known and most graphic examples of self-organization, i.e., the formation of stable, regular spatial–temporal structures in nonequilibrium dissipative media, are Bénard cells in a thin layer of liquid with a temperature gradient along the normal or ring and spiral structures in a planar chemical reactor with a gradient in the liquid-reagent concentrations. In both examples, the liquid media are initially uniform, and microscopic elements such as atoms and molecules participate in self-organization. These 'elements' diffuse in the course of their motion in space. A multidomain magnetic medium differs dramatically from the above examples. Such a medium is initially nonuniform: the direction of the vectors $\mathbf{J}_s$ in adjacent domains are opposite (the 'black' and 'white' domains in Fig. 1a); macroscopic formations (domains) participate in the self-organization process; finally, there is no diffusion in this process, no displacements of individual atoms (if we ignore the magnetostriction effects on the microscopic level). In view of what has been said, a multidomain magnetic medium should be classified as an entirely new, i.e., previously not studied, object of synergetics.

The special state of multidomain IG films described above (Figs 2, 3, 5, and 6) remarkably resembles an excited state of a self-oscillating active medium, while ring and spiral domains resemble ring and spiral dissipative (autowave) structures in, say, chemically active media [9]. Hence, in our earlier works [4–7] we stressed this analogy, calling this newly observed special excited state of a multidomain medium an autowave state. However, already in Ref. [8] we pointed out that ring and spiral dynamic domains differ dramatically in their properties from autowaves. For instance, the latter annihilate in collisions, while SDs interact rather like elastic, easily deformable, or, on the contrary, rigid formations. Figures 3, 5, and 6 clearly show this.

There are also other differences. For instance, single dynamic SDs with long rectilinear ends have been observed. What makes these SDs so remarkable is that in each of them the spiral twists and untwists along this end (which acts as a guide) and oscillates in this way in the course of its entire life. When there is a system of two coupled spiral domains of this type, one spiral twists while the other untwists, and vice versa. This continues for a time T_g. Such behavior has no known analog in the behavior of spiral autowaves [9]. Finally, we note that autowave structures vanish if the pumping of the system with energy ceases and the reasons for the formation of spatial–temporal ordered structures, such as temperature gradients in liquids and concentration gradients in chemical solutions, disappear. In our case, multiturn SDs may be conserved even if the ac field is suddenly switched off [25]. Dikshteĭn et al. [11] give several reasons why ring and spiral dynamic domains cannot be interpreted as autowave structures. They classify them as metastable, reflexive, structures.

Taking all this into account, in Ref. [8] we called a state that appears in a multidomain medium placed in an ac magnetic field and is accompanied by self-organization in the system of moving domain walls (formation of ordered, stable DDSs) and self-generation of quasi-periodic processes with a frequency much smaller than the pump frequency (appearance $\Leftrightarrow$ disappearance, emission, or generation, of dynamic domains) an 'anger' state (AS), meaning an exasperated, or angry, state. It is only logical then to call the ordered DDSs that emerge in this state magnetic 'anger' structures [51].

The important dynamic parameters of an 'anger' state are the lifetime T_g of a spiral domain and the wait time T_w within the monitored section of the sample 1–1.5 mm long. In Figs 6d and 6e, we have depicted (see Ref. [8]) curves representing the dependence of T_g and T_w on the frequency f of the ac field for values of H_0 that approximately correspond to the middle of the AS region in Fig. 2c. The solid curves represent the values of T_g and T_w averaged over 15 spiral domains, and the dashed curves represent the measured maximum values of these parameters. Clearly, $T_g(f)$ is a nonmonotonic function and $T_w(f)$, a monotonic function. As f increases and becomes higher than 300 Hz, both T_g and T_w decrease, first fast and then more slowly. For $f \geqslant 1$ kHz, $T_w \to 0$; in other words, the observed section of the film does not remain free from spiral domains. We were able to build the T_g vs. H_0 dependence for an IG film with a typical dynamic spiral domain as the one shown in Fig. 4. The $T_g(H_0)$ curve is nonmonotonic, and the peak value of T_g, equal to 30 s, is located at $H_0 = 40$ Oe with $f = 500$ Hz. Thus, exit from the AS region may be achieved by reducing the number of turns in the SDs (see Section 3) and reducing their lifetimes. It has been noticed that, all other things being equal, the larger the outer size of the spiral, i.e., the greater the number of turns in it, the longer it 'lives.' Experiments have shown [8] that the functions $T_g(f)$, $T_g(H_0)$, and $T_w(f)$ are very sensitive to the temperature and the shape of the field $H(t)$.

The dynamic SDs in the same sample and the more so in different samples differ not only in their configuration parameters (see Section 3) but also in their behavior in an ac field. In the course of its life, a spiral domain interacts with a continuously transforming ('live') disordered DDS and, due to this interaction, the number of turns and their shape may change and from time to time the core may 'pulsate,' which causes the SD to twist and untwist. The spiral is not motionless, it drifts and in the process collides with point and extended defects, with ends and outgrowths of stripe domains, with CDs, and with other SDs. In a film with fairly low uniaxial anisotropy ($Q = 9$), spiral domains can easily be deformed (Figs 2b and 6), they flow around defects, and the SD turns move so close together that the distance between them becomes of the order of the double width of reversed domains in a static field equal to the amplitude of the ac field. This means that the domain walls do not move under reversal of the magnetic field in such confluence regions. A similar picture is observed for the collision of two SDs with equal (Fig. 6b) and unequal (Fig. 6c) topological charges q.

The spiral domains in a highly anisotropic film ($Q = 96$) are more 'rigid,' with the result that compression of the outer

turns of the SDs is almost imperceptible (Figs 3c – 3e). Strictly speaking, experiments with SDs whose shapes resemble the spiral of Archimedes (Fig. 4) have shown [25] that the distance between turns depends on the turn's number and that the nature of this dependence changes dramatically as the frequency f increases. A general law has been recorded here: when the frequency is high, a close-packed lattice or mosaic of SDs is formed (say, as the one depicted in Figs 5c and 9b), the inner region near the SD core is looser than the periphery. Note that during all the changes in shape, size, and position of a spiral dynamic domain in the course of the spiral life, the sign of its topological change remains the same.

Video-microfilming [51] made it possible to study in detail the evolution of individual SDs in an IG film, whose typical dynamic SDs are shown in Fig. 3. It was found that an SD wanders in a disordered DDS (in domain chaos) just like a Brownian particle. The instantaneous velocities of these domains change in direction and in magnitude from zero to $5-6$ mm s^{-1}. We were able to follow the 'life' of a single (or what is known as isolated) SD in whose neighborhood no other SDs appeared over a period of T_g, i.e., the observed SD spent its entire life being surrounded only by domain chaos. In the first stage of its life, the emerging double-turn SD (the process took about 0.04 s, which amounted to the time between two adjacent frames in video-microfilming) was found to transform in a period of $T_b = 0.04$ s into a multiturn SD with 10 turns of the same polarity. The increase in the number of turns was achieved through the twisting of the turns, i.e., through the motion of the head of the outer turn. After that, the dynamic SD lived for about $T_g = 0.48$ s, the number of turns increased, dropped, again increased, etc.; this number N varied in a random manner, not dropping below 4 or 5. During T_g, the size of the core in the SD, the period in the turns of the spiral, and the topological charge did not change. This is followed by a stage of SD aging and destruction: the turns become more and more distorted, their number decreases, and the spiral becomes loose (especially at the center). Finally, it takes another 0.04 s for the SD to be completely destroyed, and it disappears.

On the basis of such observations, to the already known characteristics T_w (the wait time) and T_g (the SD lifetime) we added two new characteristics, the building time for a multiturn SD T_b and the SD aging and destruction time T_d. For the film used in the experiments, at $f = 2.56$ kHz and $H_0 = 43$ Oe, the values of T_g and T_d averaged over 15 spirals on an area of 10 mm^2 amounted to approximately 1 s, while the averaged values of T_b and T_d amounted to approximately 0.04 s. At the same frequency but a different field strength $H_0 = 45.7$ Oe (near the upper boundary of the AS region in Fig. 3f), $T_g = 1.5$ s, while T_w increases dramatically and reaches $10-15$ s. The latter is an indication of a mechanism of AS destruction that differs from the one established earlier in Refs [8, 25]. Indeed, in Refs [8, 25] it was found that large long-lived SDs with a large number N of turns form in the middle of the AS region, while as the amplitude H_0 approaches the upper or lower boundary of the AS region, the spiral become smaller, they have a shorter life, contain a decreasing number of turns, and finally completely disappear. This is a characteristic feature of films with a moderate Q factor ($Q \leqslant 20$).

The situation is quite different for the highly anisotropic sample ($Q = 96$) considered here. Small SDs with small values of N and T_g do form at the lower boundary of the AS region. As the field amplitude grows, N and T_g only increase, but the wait time T_w for the emergence of large (with more than $10-15$ turns) long-lived SDs increases greatly and, we believe, tends to infinity. Probably, such a difference in the AS destruction mechanisms in different films stems from the fact that in highly anisotropic substances jumps in magnetization play an important role in the course of magnetization reversal, especially at the initial stage (see Sections 7 and 8). When the amplitude of the ac field is close to the upper boundary of the AS region (Fig. 3f) and hence to the saturation field strength H_s, a low number of small residual domains of the reverse magnetic phase are retained in the film. As the field strength decreases, the growth of these domains occurs with a large hysteresis and is accompanied by large jumps of magnetization. In this way, say, in an 'appropriate' residual magnetic CD, the transition to the dumbbell-shaped and then the stripe domain occurs suddenly, and at the end of this process the velocity of the domain head is so high that the gyrotropic force (3.2) is capable of twisting the stripe domain into a spiral. An increase in H_0 leads to fewer and fewer residual domains in the system, and the probability of growth of an 'appropriate' domain drops, which means that the wait time T_w increases.

The 'anger' state is realized within a certain region of the ac field limited in amplitude and frequency (Figs 2c and 3f). The lower (threshold) frequency f_b can be estimated by assuming that the gyrotropic force (3.2) is crucial in the formation of dynamic SDs, while the position of a domain wall, e.g., the coordinate X, varies with time in the same way as the field does, i.e., $X(t) = X_0 \sin(2\pi f t)$. Then, with $H_\sim = H_0 \sin(2\pi f t)$, the domain-wall velocity is

$$V(t) = 2\pi X_0 f \cos(2\pi f t)\,,$$

or

$$V(t) \sim f \cos(2\pi f t)\,. \tag{4.1}$$

Since expression (3.2) for the gyrotropic force F_g contains V, the frequency f must obviously be higher than the minimum value f_b for the gyrotropic force to be able to twist the head of the growing stripe domain into a multiturn spiral. The fact that there is also a maximum frequency f_{max} limiting the AS region (for the films that were studied, this frequency is $6-30$ kHz) is related, most likely, to the more complex dynamics of domain walls, i.e., to the transformation of their internal structure.

The qualitative explanation [53] of the existence of an interval of amplitudes of the ac field

$$\Delta H_\sim = H_{0(\max)} - H_{0(\min)}$$

optimum for the formation of dynamic SDs is based on allowance for gyrotropic forces and the density of domains in the domain ensemble. According to equation (4.1), when the field amplitude $H_\sim = H_0$ is small, $V = 0$, which means that $F_g = 0$, provided that all the other parameters in (3.2) remain constant. Maximum velocities $V = V_0$ and, hence, maximum gyrotropic forces F_g occur when the field strength passes through zero. This is the most unfavorable situation for the formation of a multiturn SD, since at such moments there is a dense ensemble of magnetic domains in the sample. Thus, for the formation of dynamic SDs the velocity V must be high and the domain surroundings must be fairly loose.

As a first approximation for the quantitative characteristic of the looseness of a DDS ensemble, we took the effective period P of the structure. We assumed that in the quasi-static

approximation the function $P(H)$ on a quarter of the field period coincides with that calculated in Ref. [21]. This leads to the introduction of the following parameter:

$$\beta\left(\frac{H}{H_0}\right) = \frac{P(H)}{P_0}\,\frac{V(H)}{V_0}\,, \qquad (4.2)$$

where P_0 is the effective period of the domain structure at $H = 0$, i.e., in the initial demagnetized state, and V_0 is the amplitude value of the velocity. The parameter β characterizes the conditions favorable for the formation of dynamic SDs. This determines, in the given approximation, that part of the period of the ac field and hence that interval ΔH of strengths of the operating field for a given frequency f within which the formation of spiral domains is most likely to occur. We found that

$$\Delta H = (0.85 - 0.60)H_s\,,$$

which is in good agreement with the experimental data [53]. The interval ΔH normalized to $4\pi J_s$ practically coincides with the interval of SD stability under quasi-static conditions calculated by Borisov and Yalyshev [15].

In Section 3, we already noted that even low bias fields may have a profound effect on the topological charge, the geometric parameters, and the behavior of spiral domains. Further studies revealed even more striking results. It was found that in samples of IG films in which initially there were no 'anger' states, the superposition on the ac field $H_\sim = H_0 \sin(2\pi ft)$ of a sufficiently high dc bias field exceeding H_0 ($H_b \geqslant H_0$) may lead to the emergence of such a state. We called such a state an induced 'anger' state, or IAS. In the space of the three controlling parameters H_0, f, and H_b there may be several limited IAS regions. The spiral domain in these regions differs in configuration and dynamic properties, while the induced 'anger' states differ in their dynamic parameters T_g, T_w, f_b, f_{max}, and ΔH_0 [52, 53].

Actually, in addition to the above factors, there are many other physical factors that influence the formation of ordered dynamic domain structures (and SDs, in particular) of different geometries and with different parameters within a specified amplitude – frequency region of the ac field. Among these are the thickness and degree of perfection (uniformity) of the microstructure of the film sample and the characteristics of the material; the internal structure, coercivity, and mobility of the domain walls; and the special features of the disordered (chaotic) dynamic domain structure from which the spiral domains are formed and which magnetostatically interacts with an SD during its entire life. At present, it is difficult to predict which of these factors and under what conditions will play the leading (or secondary) role. For instance, it can be assumed that at low frequencies ($f \approx 0.1-1$ kHz) the coercivity of the domain walls will strongly affect the dynamics of the domain structure, while at high frequencies ($f \approx 10-100$ kHz) the transformation of the internal structure of the domain wall will influence the dynamics. However, new reliable experimental data are needed to arrive at firm conclusions. The existing theories of autowave processes and the dynamical theory of pattern formation (e.g., see Refs [9, 54, 55]) provide no ready schemes for describing the 'anger' state. The building of a thorough theory of strongly excited ('anger') states of multidomain magnetic media constitutes a complicated physical problem.

5. Leading centers and other sources of dynamic domains. The dynamic single-domain state

The above results hold for a frequency range $f \sim 0.1-10$ kHz and amplitudes H_0 smaller that the static saturation field H_s. Extending these intervals to the frequency $f = 100-150$ kHz and to the amplitude H_0 of the ac field to $(2-3)H_s$ has led to the discovery of many new stable, ordered DDSs and new effects in their behavior.

When H_0 is higher than the saturation field H_s, local defects begin to play a substantial role in highly anisotropic IG films ($K > 2\pi J_s^2$): microscopic domains with magnetizations opposite to that of the film magnetization taken almost to the saturation value are preserved or form around these defects. If the field strength is reduced to values below H_s, some of these reverse-magnetization microdomains grow and initiate magnetization reversal in the entire film by displacing the domain walls, i.e., become magnetization-reversal nuclei. Dislocations and aggregates of dislocations may serve as such defects. According to Vlasko-Vlasov et al. [56] and Nikolaev [57], near a dislocation the effective constant of uniaxial magnetic anisotropy may not only rapidly decrease but even change sign.

Within the adopted experimental setup considered (see Section 2), it was found that ordered stable DDSs form in the investigated IG films at certain values of the frequency and amplitude of the ac field $H = H_0 \sin(2\pi ft)$. We called these DDSs leading centers (LCs) by analogy with similar spatial – temporal ordered dissipative structures in active media [9]. An LC is a DDS in the form of a system of concentric rings propagating away from the center with moderate velocities (Figs 7a – 7c). Here, the pattern observed in a microscope is very similar to the propagation of circular concentric waves. The formation of such structures stems from the continuous periodic nucleation and growth of magnetic CDs of alternating polarity near a local defect [58 – 60]. The process causes the entire system of rings to drift away from the center. (The reader interested in a detailed discussion of the drift of an aggregate of domains as a whole in IG films can find it in Ref. [14].)

Recently, we were able to observe, using video-microfilming, a different mechanism of LC formation: first a single-turn dynamic single domain appears at a defect, then the number of turns in the SD increases, and finally the turns suddenly merge (this takes less than 0.04 s), and a system of concentric ring domains (CRDs) is formed. Presumably, this transition occurs via the formation and motion of a domain dislocation [11, 61], in the same way as concentric circular waves transform into spiral waves in a system of parametrically excited capillary (ripple) waves in a thin layer of liquid [55].

The natural frequency f_s of 'operation' of an LC (the production of rings) is several orders of magnitude lower than the pump frequency ($f_s \ll f$) and amounts to 0.1 – 1 Hz. For the given H_0 and f, an optimum number of rings N is reached (Fig. 7c). Further, as time passes, this number remains practically constant: each 'nucleation' of a CD corresponds to a shift (or drift) of the entire system of rings from the center outwards accompanied by destruction of the peripheral ring. The latter occurs, as Figs 7a – 7c show, through a nonuniform expansion of the outer ring and formation and detachment of an irregularly shaped domain — a large 'bubble.' The accompanying increase in the magnetostatic energy is balanced by the emergence of cylindrical domains (CDs) inside such a bubble. The process

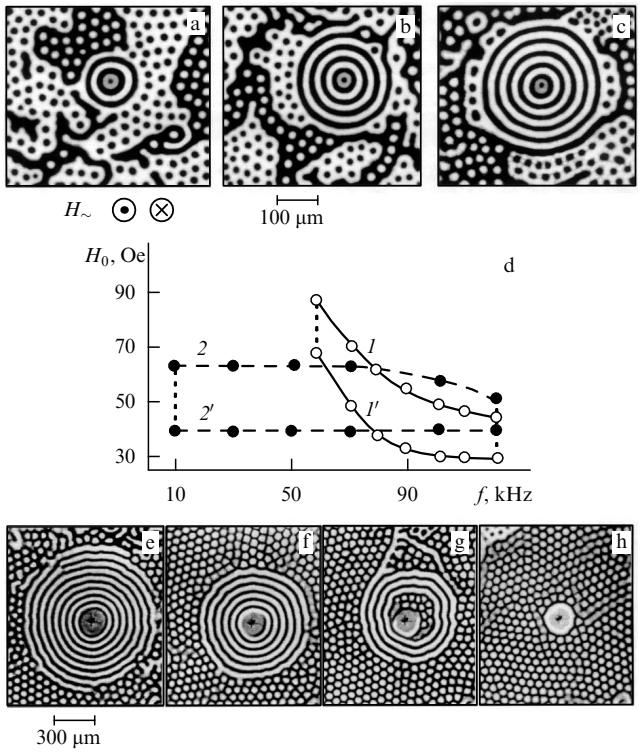

Figure 7. (a, b, and c) Dynamic domain structure of leading-center type in a $(YBi)_3(FeGa)_5O_{12}$ film with $L = 9$ μm, $P_0 = 32$ μm, and $Q = 53$ placed in a field $H_\sim$ of frequency $f = 80$ kHz and amplitude $H_0 = 58$ Oe at 40 °C (the frames are separated in time by 30 s). (d) The amplitude–frequency regions where the LC operates at 30 °C (curves *1* and *1′*) and 65 °C (curves *2* and *2′*). (e, f, g, and h) LC destruction by a dc bias field H_b equal to (e) 0, (f) 2, (g) 4, and (h) 7 Oe at $f = 80$ kHz and $H_0 = 64$ Oe.

is repeated many times. As a result, the leading center finds itself surrounded by a disordered DDS consisting of white and black bubbles of various shapes with, respectively, black and white cylindrical domains inside. (Such a bubble with cylindrical domains inside can also be called a cluster of CDs of this or that polarity.) The entire system is in the state of violent and disordered motion.

Note that the formation of white and black clusters containing cylindrical domains (Figs 7a–7c) occurs with equal probability, and the total areas occupied by these types of clusters are approximately the same. However, even a small (0.2–0.5 Oe) dc component in the ac field lifts the degeneracy up to a point were the LC finds itself surrounded by a lattice of cylindrical magnetic domains of the same polarity (e.g., see Fig. 7e). We believe that the ordered LC structure with different disordered DDSs surrounding the LC can strongly affect the dynamic and configuration parameters of the LC, i.e., the natural frequency f_s, the number of rings N, and the ring width d.

Figure 7d shows the amplitude–frequency $(H_0 - f)$ regions of existence of leading centers for two temperatures. Clearly, temperature has a very strong effect on these $(H_0 - f)$ regions. Different IG film samples exhibit different $(H_0 - f)$ regions of operation of leading centers and different behavior of these regions under temperature variations, due not only to the different temperature dependence of the main magnetic constants of the material but also to the temperature dependence of the local characteristics near a defect, where the magnetization-reversal nuclei appear.

A dc bias field H_b has no less an effect than temperature on a leading center. Figures 7e–7h show how an increase in the field strength H_b leads to gradual destruction of a leading center for the given values of the parameters of the ac field. What is important here is that the destruction proceeds in two stages: first, the outer (white in Figs 7e and 7f) rings successively decay into chains of CDs, and this is followed by the formation of bubbles at the LC center (black in Fig. 7g) with white CDs inside. As a result, the LC disappears, while the defect region finds itself surrounded by a unipolar lattice of 'white' magnetic bubbles (Fig. 7h). When the sign of the field H_b changes, the polarities change to the opposite ones.

Thus, within limited regions of f and H_0, there forms an excited state of iron garnet films whose characteristic feature is the formation of ordered, stable DDSs (systems of concentric rings), i.e., what we observe is self-organization of an ensemble of domains and the presence of a periodic emergence–disappearance process. In Section 4, we defined such a state as the 'anger' state (AS) of a multidomain medium. Probably, we may assume that the formation of SDs and LCs is the manifestation of the same phenomenon, the emergence of a strongly excited ('anger') state of an ensemble of interacting magnetic domains, and that the AS manifests itself differently, depending on the experimental conditions. What comes to mind as an analog of such operation of LCs in films with perpendicular anisotropy is the effect first observed in samples of transformer steel (Fe–3%Si) with the EA parallel to the sample plane and to the observed surface [1, 62]. In an ac magnetic field ($f = 60$ Hz), a planar domain periodically appears near a local defect and grows with a frequency of about 0.5 Hz. This causes the entire system of planar domains to drift to the edge of the sample.

Experiments have shown that variations of the pump parameters, i.e., the frequency f and amplitude H_0 of a sinusoidal ac field, dramatically change the shape of DDSs in highly anisotropic IG films (Fig. 8) [63]. For instance, multiprong 'stars' form near defects (Fig. 8a). Due to the elongation $\Leftrightarrow$ shortening of the prongs, the stars constantly 'blink' with a frequency $f_s \sim 1$ Hz, which is several orders of magnitude lower than the frequency f of the ac field. The length of the 'prongs' depends on H_0 and f, so that under an appropriate variation of these quantities this length may decrease. Finally, at certain values of H_0 and f the 'stars' disappear and the entire sample becomes a single domain, which means that it ceases to react to the external ac magnetic field. In this case, we say that a dynamic single-domain state has set in. We will discuss this state in Sections 6 and 7 devoted to dynamic domain phase diagrams and the hysteresis properties of IG films. We also note that large defects, which can be observed in Fig. 8a, have been specially produced on the sample by a diamond indenter of a device for measuring microhardness. Small defects are of natural origin — they are present in the sample from the very beginning. Such 'marking' has made it possible not only to observe DDSs many times at the same place of the sample (e.g., see Figs 8a–8d) but also to make certain that the main features of the configuration and dynamic behavior of the structures described in this section are the same for DDSs that form around artificial local defects and for DDSs that form on natural 'conditional' point defects.

For certain values of the two parameters of the ac magnetic field, H_0 and f, the defects may becomes sources of DDSs in the form of bubbles (clusters and islands) filled with CDs (Fig. 8c). How such 'large bubbles' may arise can

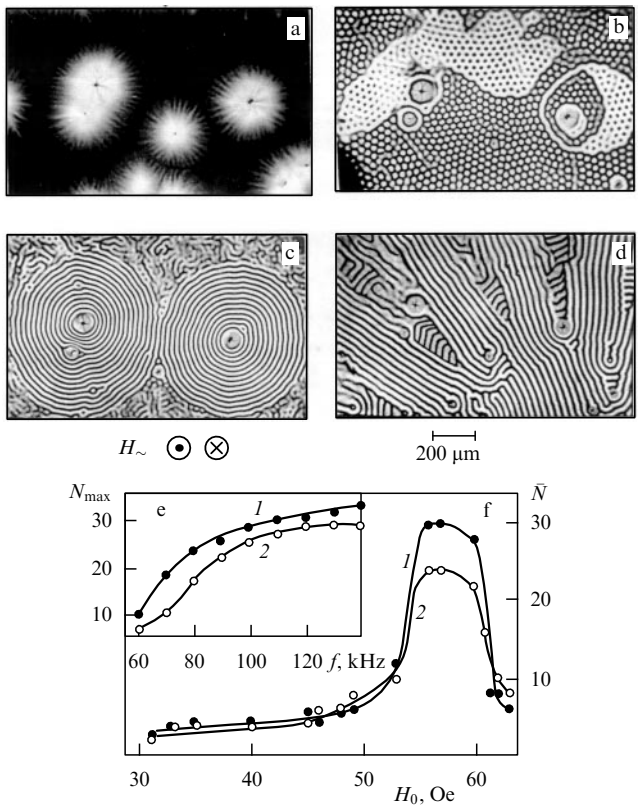

Figure 8. Different types of DDSs in the same film as in Fig. 7 at different frequencies and amplitudes of the field $H_\sim$: (a) 'blinking stars' (10 kHz, 82 Oe); (b) sources of bubbles (70 kHz, 72 Oe); (c) domain centers (100 kHz, 60 Oe); and (d) a radial–circular structure (100 kHz, 80 Oe). (e) Dependence of the time-averaged number of ring domains in a domain center on the amplitude of the ac field $H_\sim$ at $f = 100$ kHz. (f) Dependence of the maximum number of rings on the frequency f (curves *1* refer to the left-hand domain center; and curves *2*, to the right-hand domain center in figure c).

clearly be seen in Fig. 8b (the large right-hand defect). Here, the inner white ring domain has only started to nonuniformly expand, with the first three black magnetic bubbles beginning to form in it. The black domain that had appeared before this all happened has expanded to such an extent that it contains many white CDs. And the white outer ring domain, which had appeared even earlier, transformed into a white bubble filled with black CDs with a white arc encompassing the source. The next moment the arc is broken and an isolated white bubble (containing black magnetic bubbles) is formed, which drifts to the edge of the sample and disappears there. The cluster of white CDs inside a black ring merges with the lattice of CDs surrounding the defect. All these stages are repeated over and over (with a frequency $f_s = 0.1-1$ Hz) as long as the experimental conditions (the frequency, amplitude, shape of the pump magnetic field, and temperature) do not change, but the configuration and size of the bubbles change in a random manner (e.g., see the irregular bubble to the left of the large defect in Fig. 8b).

Within certain intervals of values of the parameters H_0 and f of the magnetic field, local defects may become centers of very large (with an outer dimension of 2–3 mm) systems of CRDs (e.g., see Fig. 8c), These domains, called *domain centers*, are similar to a leading center but here no periodic generation of cylindrical and ring domains at the center of the system is observed and hence no propagation of rings from the center to the periphery occurs. For constant f and H_0, the number of rings N in domain centers remain practically the same with the passage of time. The domain walls only oscillate near stable positions of equilibrium. When f and H_0 change, the number of rings in domain centers changes via growth or destruction of the outer rings. The dependence of N on the field amplitude (Fig. 8e) is essentially nonmonotonic; N_{max} is realized in a fairly narrow range of amplitudes, $H_0 \sim 55-60$ Oe. This is the optimal interval of dynamic stability of a system of CRDs at $f = 100$ kHz. As the frequency grows, the value of N_{max} steadily increases, as Fig. 8f clearly shows.

In another sample, whose domain structure is shown in Fig. 3, we observed stable dynamic structures of CRDs with $N_{max} > 50$ in an ac harmonic field with $f = 100$ kHz and $H_0 = 75$ Oe. These were huge CRD systems occupying the larger part of the sample. Such a structure can be retained even after the ac field is switched off. The behavior of these CRD systems in dc magnetic fields is extremely interesting [64]. Under magnetization, the rings in such systems move one after another to the center and disappear at some critical values of the radius R_{cr} and the field strength H_{cr}. Here, larger values of H_{cr} correspond to larger values of R_{cr}. Interestingly, the outer rings in a CRD system exist up to field strengths almost twice as high as the field strength for magnetic bubble collapse (i.e., the field strength H_s) for a given sample. To our knowledge, such naturally emerging, anomalously stable huge CRD systems have been observed for the first time in [64]. In Ref. [64], the stability and properties of a CRD system were also studied theoretically and the expression for the total free energy of a CRD structure with an arbitrary number of rings [65] was employed. A new parameter, the coercivity of a ring domain, was also introduced. This parameter was defined as the difference of the derivatives of the total energy with respect to the outer and inner radii of the rings. It was found that the theory provides a satisfactory description of the CRD properties, including the effect of the anomalously high stability of huge CRD systems in static fields.

It should be noted that huge CRD systems can be formed, as shown in Ref. [66], in iron garnet films artificially by applying a high-intensity microwave field (such a field can be generated by a special circuit of waveguides) in addition to the dc bias magnetic field.

Now, let us return to the DDSs shown in Figs 7 and 8. As noted earlier, in a leading center, the ring domains move from the center to the periphery, while in a domain center, no motion of this type exists. Along with such DDSs, within certain intervals of frequencies and amplitudes of the ac field we were able to observe an ordered DDS (as well as a leading center and a domain center) consisting of a system of concentric ring domains in which the rings slowly and periodically moved to and from the 'center' one after another. We called such a DDS an *elastic domain center*. Presumably, such a center by its very nature occupies an intermediate position between a leading center and a domain center. It cannot be ruled out that an elastic domain center appears when the frequency of operation of the leading center becomes close to the natural frequency of oscillations of the local density of the dynamic domain ensemble surrounding the leading center. When the parameters of the pump field are varied and huge CRD systems are formed, all group motions of rings are hindered, and the system passes into the domain-center state. We will call all the above-described domain structures 'leading-center-type' (LC-type) structures.

We also note that in the same section of the sample under consideration (see Fig. 8) but at a somewhat higher temperature (39 °C) we observed [63] an amazing radial–circular dynamic structure (Fig. 8d). Unfortunately, so far this structure has received very little attention from researchers.

Thus, as the parameters of the ac field change, a whole set of transformations of the dynamic domain structure that forms at one and the same local defect are realized (Figs 7 and 8). Here, the mutual transitions between the above structures may occur with a noticeable hysteresis. At the same time, under given conditions different DDSs of the leading-center type may form in the film around different defects (these DDSs also interact with each other). For instance, the formation of domain centers on two large defects (Fig. 8c) leads to suppression of the leading center on a small defect located between the two large defects.

At present, there is no detailed theory of the entire set of the phenomena described in this section. However, there are solutions of a number of particular problems, which we will briefly discuss now.

The first properties studied both experimentally and theoretically were those of a ring domain [67–69]. Several interesting features were established. For instance, in a sawtooth ac magnetic field of a very low frequency (lower than 1 Hz), the inner wall (radius R_1) and the outer wall (radius R_2) of a ring alternatively move toward the center with a large phase shift. Here the destruction of the ring domain may occur in different ways: through a collapse with the values of R_1 and R_2 remaining finite, through thinning-down of the ring, i.e., $R_2 - R_1 \to 0$, or through a transition to a CD.

The problem of theoretically describing magnetic DDSs of the leading-center type was formulated in Refs [65, 70–76]. The first attempt to establish physically justified approaches to calculations of the amplitude–frequency region of existence and operation of a DDS of the leading-center type was made in Ref. [70].

Gal'tsev and Yalyshev [71] used a model in which a single CD was surrounded by a ring domain of the same polarity to solve the complicated micromagnetic problem of finding the continuous radial distribution of magnetization corresponding to the minimum of the total energy density equal to the sum of the energy densities corresponding to anisotropy, exchange, magnetostatic interaction, and the Zeeman effect. Although the researchers examined the static case, by analyzing the possible ways of the appearance $\Leftrightarrow$ disappearance of a ring domain, they concluded that, theoretically, several concentric rings may form around a CD when the system is excited and operates as a leading center.

The same researchers also employed the above model under dynamic conditions [72, 73]. They analyzed the reaction of a domain structure consisting of three domain walls with radii R_1 (a cylindrical domain) and R_2 and R_3 (a ring domain) to a pulse of a magnetic field directed against J_s in the domains. What was found was that, depending on the amplitude of the pulse, the wall system moves either toward the center (compression and collapse) or away from the center (expansion). The range of field strengths in which the nature of wall motion changes is extremely narrow and, as the researchers believe, determines the field interval in which the lifetime T_g of the system is extremely large at a certain value of the field strength $T_g \to \infty$; i.e., the entire structure becomes dynamically stable. The calculated dependence of T_g on the pulse amplitude is similar in shape to the $T_g(H_0)$ dependence found in experiments for dynamic SDs [8, 46]. Gal'tsev and Yalyshev [72, 73] also studied the behavior of a system consisting of a magnetic bubble and a ring domain in a sawtoothed oscillating field. They postulated that domain-wall vibrations follow the field oscillations and that the change in the size of the domains is determined by the dc component of the field. The result was a theoretical substantiation of the behavior of the walls of a ring domain observed in the experiments of DeJang et al. [68] and Antonov et al. [69].

Mal'tsev et al. [65, 74–76] examined a system consisting of an arbitrary number of CRDs placed in a dc or ac harmonic magnetic field. Using an approximation in which the domain-wall thickness is zero and the domain magnetization is uniform, the researchers derived an expression for the total energy density of a CRD system and studied the stability of such a system and the effect on this stability of a central local defect in the form of a small magnetic bubble with an irreversible magnetic moment [65]. The analysis of the properties of the DDS of the leading-center type is based on a phenomenological dissipative model. It is assumed that in the course of the motion of ring domains, the domain walls are subject to two types of force, the friction force proportional to the velocity of motion (viscous friction) and the friction force generated by the interaction of walls with different types of nonuniformity (the coercive force), and that the entire energy pumped by the external field into the system is spent on the motion of the domain walls.

The equations of motion of the wall of any ring domain can be found by solving the Lagrange equation, which incorporates the potential energy U and the kinetic energy T of the system. When reduced to $(2\pi J_s)^2 L^3$, these energies can be written as follows:

$$U = 2\tilde{l}\sum_{k=1}^{N} R_k - h(\tau)\sum_{k=1}^{N+1} s_k R_k^2 + \sum_{k=1}^{N+1} s_k R_k^2 + \int_0^\infty \frac{1-\exp(-x)}{x}\left[\sum_{k=1}^{N+1} s_k R_k J_1(R_k x)\right]^2 \mathrm{d}x\,, \qquad (5.1)$$

where N is the total number of ring walls in the CRD system; $R_k = r_k/L$ is the reduced radius of the kth wall; $\tilde{l} = l^*/L = \gamma/(2\pi J_s^2 L)$ is the reduced characteristic length; L is the thickness of the film; J_s is the spontaneous magnetization; γ is the surface energy density of a domain wall; $h = H/(4\pi J_s)$; $\tau = t\omega_0$ is the dimensionless time; $\omega_0 = 2\pi f$ is the circular frequency of the ac field;

$$s_k = \begin{cases} 2(-1)^k, & k \leqslant N, \\ \rho - (-1)^N, & k = N+1, \end{cases}$$

$\rho = J_{def}/J_s$ is the magnetic charge of the defect; J_{def} is the defect magnetization; J_1 is the Bessel function of the first kind and first order; and

$$T = \frac{L m_D \omega_0^2}{4\pi J_s^2}\sum_{k=1}^{N} R_k\left(\dot{R}_k\right)^2, \qquad (5.2)$$

where m_D is the Döring effective mass of a domain wall. In terms of these variables, the equation of motion for the kth wall is

$$\beta_1\left(\ddot{R}_k + \frac{1}{2R_k}\left(\dot{R}_k\right)^2\right) + \beta_2\dot{R}_k + 2h_c\,\mathrm{sgn}\left(\dot{R}_k\right) + F_k(R_k,\tau) = 0\,, \qquad (5.3)$$

where

$$\beta_1 = \frac{L}{\Delta_0}\left(\frac{1}{4\pi\tilde{\gamma}J_s}\right)^2(1+\alpha^2),$$

with $\Delta_0 = \sqrt{A/K}$ (A is the exchange interaction parameter and K is the uniaxial anisotropy constant), α is the viscous damping parameter, $\tilde{\gamma}$ the effective gyromagnetic ratio;

$$\beta_2 = 2\frac{L}{\Delta_0}\left(\frac{1}{4\pi\tilde{\gamma}J_s}\right);$$

$$F(R_k,\tau) = \frac{\tilde{l}}{R_k} + s_k\left[1 - h(\tau) + \int_0^\infty \frac{1-\exp(-x)}{x} J_0(R_k x) \times \sum_{n=1}^{N+1} s_n R_n J_1(R_n x)\,\mathrm{d}x\right],$$

with J_0, the Bessel function of the first kind and zeroth order, and x, the radial coordinate. Estimates [74] of the parameters β_1 and β_2 for the iron garnet films under investigation have revealed that β_1 is several orders of magnitude smaller than β_2. Hence, in the first approximation, the term with β_1 in (5.3) can be dropped, i.e., inertia effects can be ignored. Further simplifications of the theoretical model amounted to excluding the coercive force h_c and the defect at the center of the CRD system. The latter simplification means that the existence of a leading center stems primarily from the dynamic stability of the CRD system proper rather than from the special features of magnetization-reversal processes on the defect (the effect of the defect on the emergence and operation of the leading center constitutes a separate, extremely complicated problem). We then have the following equation for computer calculations:

$$\beta_2\dot{R}_k + F_k(R_k,\tau) = 0. \qquad (5.4)$$

The solution of this equation yielded a graphic (in the form of diagrams) time dependence of the radius of the ring domain walls, which showed that, after the field is switched on and the first stable ring is formed, a certain time has to pass before the second ring becomes stable, and this situation is repeated with the third ring. (The stability criteria are studied in Ref. [74].) The domain walls vibrate with a frequency equal to that of the external field (f), and the higher the frequency f, the smaller the amplitude of the wall vibrations. While vibrating, the domain walls slowly drift away from the center; i.e., the rings expand.

In this way, the operation of a leading center was demonstrated by theoretical means. Next, Mal'tsev and Fakhrutdinov found [75] that there exists a certain threshold frequency of the harmonic field below which a CRD system is unstable. They established the upper bound on the field amplitude for the stability region of a CRD system and the dependence of this critical amplitude on the field frequency for systems with different numbers of rings. The family of the curves representing this dependence suggests that an increase in the field amplitude at $f = \text{const}$ destroys the rings and that a CRD system that is unstable at given amplitude and frequency may become stable as the frequency increases; i.e., the frequency of the ac field becomes a factor that stabilizes a DDS of the leading-center type. All the theoretical results discussed above and those discussed in Refs [71 – 75] but not mentioned here agree with the experimental data and stimulate new experiments.

We also note that the structures shown in Figs 7 and 8 do not exhaust the diversity of DDSs observed in experiments. For instance, a defect was found to be a source of small dynamic domains in the form of rings [77]; small rings were observed to detach themselves from the defect one after another. The rings were found to form a more or less ordered dynamic lattice. As in the case of a leading center described above, the source of the rings has its own region of existence in terms of the amplitude H_0 and frequency f of the ac field $H_\sim = H_0\sin(2\pi ft)$. It was found that ΔH_0 is approximately 40 – 80 Oe and Δf, approximately 70 – 120 kHz. The average maximum diameter of the rings decreases with increasing H_0 and f. The natural frequency of operation of the ring source varies nonmonotonically with the amplitude H_0, reaching its maximum value $f_s = 12$ Hz at $H_0 = 60$ Oe and $f = 100$ kHz. While the leading, domain, and elastic domain centers discussed earlier emerge on local 'conditional' point defects, ring sources emerge on defects in the form of a microscopic scratch.

A final remark, which also applies to Sections 6 – 8, is in order. After the results of the appropriate experiments have been discussed, problems of establishing the nature, size, shape, and orientation of the defects that serve as DDS centers of the leading-center type become central. It is natural to assume that the enumerated factors determine, to a greater or lesser degree, the activity of specific defects and centers of dynamic CRDs, since the mechanisms of formation and growth of magnetization-reversal nuclei in ac magnetic fields are different for different cases. Resolving these questions requires doing serious and systematic experimental work and solving complicated theoretical problems on the micromagnetic level. So far, neither of the two has received serious attention.

6. Giant dynamic domains

The dynamic domain structures (DDSs) described in the previous sections consist of concentric ring domains (the leading and domain centers in Figs 7 and 8) whose ring width ΔR is on the same order as the domain width d_0 in the initial demagnetized state or the width of stripe domains in the spiral turns. At the same time, in certain highly anisotropic iron garnet films at appropriate values of the pump parameters (H_0, f), we observed [6, 25, 46, 58, 59] extremely large (giant) DDSs of the leading-center type whose ring width was at least ten times greater than d_0. Such a giant leading center observed at $f = 50$ kHz is shown in Fig. 9a. To be more graphic and to justify the term 'giant,' in Fig. 9b we depict a DDS in the same place of the film but at $f = 5$ kHz on the same scale as in Fig. 9a.

The amplitude – frequency region ($H_0 - f$) of existence of giant leading centers at 40 °C is presented in Fig. 9d. As in the case of an ordinary LC, temperature has a significant effect on the size and configuration of the ($H_0 - f$) region. For instance, for the sample under investigation, the emergence of a giant LC is observed only when the sample is heated to 40 – 50 °C. Presumably, this is related to the necessity of thermally activating the process of formation and growth of magnetization-reversal nuclei on local defects, centers of giant LCs. Several such leading centers are generated in the specified ($H_0 - f$) region, but only one becomes the principal center. It has the highest natural frequency of operation f_s and the largest number of ring domains, $N \approx 10 - 12$. It also suppresses other LCs, since they have no more than two or three

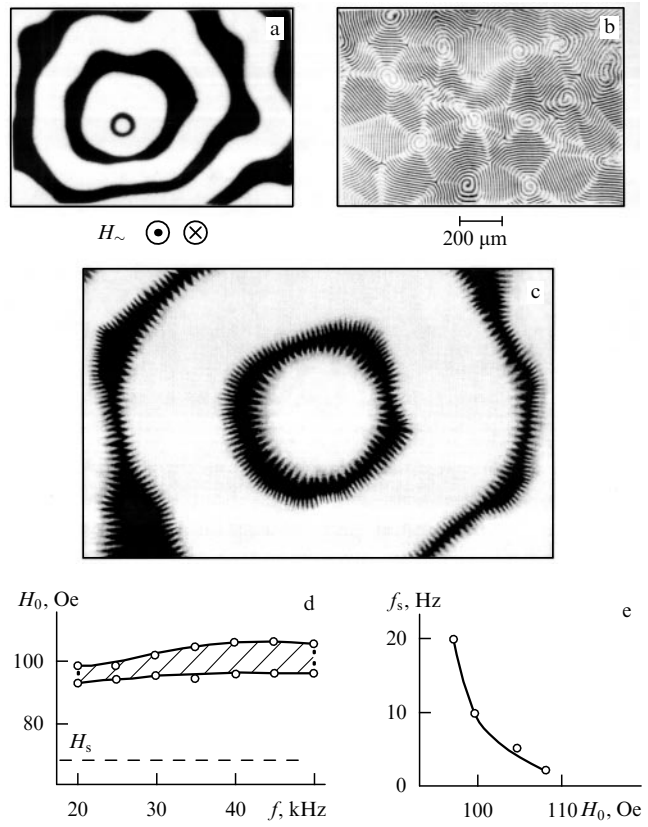

Figure 9. (a) Giant leading center observed in the same film as in Fig. 5 in a field $H_\sim = H_0 \sin(2\pi ft)$ with a frequency of 40 kHz and an amplitude of 100 Oe, and (b) an 'ordinary' ordered DDS in a field with $f = 5$ kHz and $H_0 = 43$ Oe. (c) The comblike walls of the giant leading center, (d) the amplitude – frequency region of existence of the leading center, and (e) the natural frequency f_s of operation of the leading center as a function of the field amplitude H_0.

ring domains. The diameter of the giant LC may reach 2.5 mm.

The natural frequency f_s of operation of the principal giant LC (the frequency of ring emission) is at least three orders of magnitude lower that the pump frequency f and strongly depends on the field amplitude. Figure 9e, which corresponds to the case where the field frequency is 50 kHz, suggests that the natural frequency f_s decreases rapidly as H_0 increases. So, by selecting the proper frequency f_s, we can stop the propagation of ring domains away from the center, i.e., 'freeze' a giant LC. It is in this state that this LC is shown in Fig. 9a.

Possibly, the most remarkable fact here is that the walls of the ring domains in giant LCs are shaped as combs (Fig. 9c), with the width of the teeth being approximately equal to d_0. The length of the teeth decreases $\Leftrightarrow$increases with a frequency much lower than that of the pump field. This leads to an effect discussed earlier for DDSs shaped as stars (Fig. 8a), precisely, to observable pulsations of the rings in a giant LC, which is especially evident in the 'frozen' state of the leading center (Fig. 9a). A model of a giant LC is discussed in Refs [46, 58] and the displacement of a comblike domain wall, in Ref. [78].

The $(H_0 - f)$ region where the principal giant LC exists (see Fig. 9d) is limited from the left by the minimum frequency $f = 20$ kHz and from the right by the maximum frequency $f = 50$ kHz. At frequencies below 20 kHz, DDSs shaped as huge 'blinking' spots, or 'floating clouds,' one to two millimeters in diameter, form in the sample. At frequencies higher than 50 kHz, the operation of the giant center is disrupted and intensive generation of very large magnetic CDs with a diameter greater than 50 μm sets in. Within the specified $(H_0 - f)$ region, the giant leading center is surrounded by such CDs and short stripe domains. In all these DDSs, the walls are comblike with teeth that pulsate in the ac field. As the pump frequency grows, the characteristic dimensions of the domains decrease [25]. The center of an operating giant LC is a natural conditional point defect around which ring domains form and grow one after another. Here, one can observe the propagation of the first two or three rings as proceeding in steps, from one fixed diameter to another [46]. Most likely, this is due to the sudden growth of the magnetization-reversal nucleus after it reaches its critical size.

Thus, in the amplitude – frequency region $(H_0 - f)$, Fig. 9d exhibits the specific reaction of the domain structure of the sample to an external ac field: the formation of ordered structures consisting of CRDs, and the emergence of periodic (quasi-periodic) processes with their own natural frequencies $f = 10^2 - 10^5$ (the emission of rings). According to the definition given in Section 4, such an exited state of a multidomain film can be classified as an 'anger' state.

7. Dynamic domain phase diagrams

The DDSs described in the previous sections do not exhaust the diversity of dynamic domain structures that we observed in iron garnet films placed in a continuously acting, spatially uniform low-frequency ($f = 10^2 - 10^5$ Hz) ac field (most often, this is a harmonic field). In Figures 2c, 3f, and 7d, we emphasized the amplitude – frequency $(H_0 - f)$ regions of 'anger' states while ignoring the surroundings in the (H_0, f) plane. Experiments have shown that in this area, too, there are various types of dynamic structures. Among these are ordered, disordered, and mixed DDSs.

Allowing for this fact, we built and analyzed the complete dynamic domain phase diagrams (PDs) for the investigated samples within a broad range of amplitudes and frequencies of the ac magnetic field [79, 80]. We classified the various DDSs that belong to different domain phases according to their configuration and dynamic behavior. Since the magnetic state of a sample and the domain structure of that sample may strongly depend on the sample's magnetic history, the construction of the phase diagram followed the same line in every case: the frequency f was fixed at a constant value and then the field amplitude H_0 was gradually increased, with the DDS identified only after exposure to the given f and H_0 for a time interval no shorter than 20 s. Such an approach makes it possible to assume that only dynamically stable or, in other words, dynamically equilibrium structures will be represented in the phase diagram. The results of microscopic observations were then augmented with those obtained through microfilming and video-microfilming. As a result of all these investigations, we found that phase diagrams are a goldmine of information about cooperative phenomena in dynamic magnetic-domain systems.

For example, Fig. 10 is an illustration of a phase diagram for one of the highly anisotropic iron garnet films we investigated. To make the picture more graphic, different dynamic domain phases have been depicted differently. Solid lines indicate the boundaries of rapid transitions from one

phase to another, while the dashed lines indicate the boundaries for gradual transitions. The phase diagram has been built from the results of microscopic observations of DDSs in the field $H_{\sim} = H_0 \sin(2\pi ft)$.

In regions *3* and *11*, 'anger' states are realized and ordered DDSs shaped as spirals (*3*) of DDSs of the leading-center type (*11*) form. Strictly speaking, region (*3*) should be divided into approximately three sections corresponding to the following frequency ranges: 0.2–0.5 kHz, 0.5–1.0 kHz, and 1–7 kHz. In the first section, we observed large, short-lived ($T_g < 0.5$ s) dynamic SDs with a small number of turns (two or three turns). In the second, we observed small, short-lived ($T_g < 0.1$ s) SDs with a small number of turns. Finally, in the third section, large multiturn (15–20 turns) long-lived (T_g up to 10 s) SDs are formed (see Fig. 3). It is these large spirals and the region of their existence that are shown in Fig. 3. Similarly, region *11* in the phase diagram (see Fig. 10) could also be divided into parts in which leading centers, domain centers, and sources of bubbles prefer to form. However, the boundaries of these regions are hazier than in the case of the different SDs in region *3*. (The uppermost right-hand corner of the phase diagram in Fig. 10 has not been filled due to technical limitations of the various devices used in the experiments.)

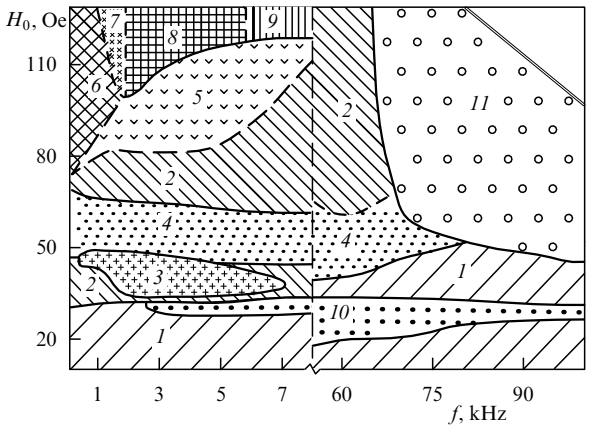

Figure 10. Dynamic domain phase diagram for the $(YLuBi)_3(FeGa)_5O_{12}$ film with $L = 9.5$ μm, $P_0 = 33$ μm, and $Q = 96$ built from the results of observations in a harmonic magnetic field. The figures in the different regions indicate the following phases: *1*, mobile labyrinth and stripe block DDS; *2*, disordered DDS ('visual chaos'); *3*, anger state (AS) and dynamic spiral domains; *4*, 'gray background'; *5*, radial DDS; *6*, radial-chaotic DDS; *7*, 'blinking stars'; *8*, dynamic single-domain state; *9*, giant dynamic domains ('floating clouds'); *10*, stripe DDS and 'islands' of heteropolar magnetic-bubble lattices; *11*, sources of dynamic domains, DDSs of the leading-center type.

The other important parts of the phase diagram are the regions occupied by *radial dynamic structures* (*5* and *6*). Here, H_0 is much higher than H_s, the static saturation field strength, which is approximately 50 Oe. Since the sample is highly anisotropic (the Q factor $Q = K/(2\pi J_s^2) = 96$), magnetization reversal begins with a sudden expansion of the residual nuclei preserved at local defects. For instance, a microscopic magnetization-reversal nucleus — a magnetic domain whose magnetization ($-J_s$) is opposite to that of the film — acts as a center from which stripe domains grow and develop in all directions in an avalanche-like manner. As a result, there emerges a radial dendritic domain structure. Such domain structures have been observed long ago (e.g., see Refs [81, 82]) in single crystals of various highly anisotropic magnetic substances subject to quasi-static magnetization reversal. The jump in magnetization and the formation of a radial domain structure occurs in a field whose strength H_K is lower than the saturation field H_s. The quantity $\Delta H_K = H_s - H_K$ or, in reduced units, $\Delta h = (1 - H_K/H_s)$ is the quantitative measure of hysteresis caused by the difficulties in the growth of residual nuclei (or, possibly, to the difficulties in the formation and growth of nuclei if no residual microscopic domains at defects were preserved).

Our experiments [81, 82] suggest that the shape of a radial DS largely depends on the magnetic history of the sample and on the maximum magnetic field strength $H_m \geqslant H_s$. For the formation of a radial DS that emerges at the center and then propagates over the entire sample (whose size is ~ 1 mm), there must be at least one real DS nucleation center and the magnetic field strength must be within an optimum field interval ΔH_K (or Δh). For instance, in the case of thin crystal plates of MnAlGe of basal orientation, the optimum value of Δh lies within 0.2–0.6, and the corresponding variation of the reduced magnetization is $\Delta(J/J_s) = 0.08$–0.4 [81]. When Δh is small, i.e., when $H_K \approx H_s$, the jump in magnetization is small and, as the field strength is gradually reduced after the jump, a labyrinthine DS is formed. When there is significant hysteresis and $\Delta h > 0.7$, many CDs and short stripe domains whose alignment is not perceptible are formed after the jump. Often it is difficult to classify such a DS as a radial DS. This fact is most likely to be an indication that the domain wall motion is not stationary and is accompanied by the formation of Bloch lines and the destruction of stripe domains on magnetic bubbles.

The time lag in the formation and growth of nuclei is the main reason for magnetic hysteresis in highly anisotropic magnetic substances and, in particular, in hard magnetic materials used as permanent magnets. A characteristic feature of this type of hysteresis is the strong dependence of hysteresis (i.e., the time lag in the magnetization jump) on the strength of the magnetizing field: the stronger the field, the greater the time lag in the jump (e.g., see Refs [34, 81–84]). Khrabrov [84] explained the H_K vs. H_m dependence by the assumption that each nucleus is characterized by two critical fields, one for the destruction of the nucleus and the other for the beginning of sudden growth of the magnetization-reversal nucleus. In Ref. [83], we introduce the idea of a spectrum of metastable states of a nucleus in which each state is realized at its own value of H_m, with a corresponding set of field strengths H_{Ki} inducing magnetization jumps. Anyhow, as H_m grows, magnetization-reversal nuclei with higher fields (energies) of activation remain suitable for the magnetization-reversal process. Filippov and Lebedev [85] examined magnetization-reversal nuclei not related to local defects. The growth of such nuclei, however, is hindered by a spatially nonuniform critical field. The calculated H_K vs. H_m dependence agrees with the experimental curve.

All highly anisotropic IG films used in our investigations exhibited the above-described features of the magnetization-reversal processes arising from the growth of nuclei. For instance [46], after magnetization in dc fields $H_m = 43, 64, 94$, and 113 Oe of a 8.6-μm thick $(LuBi)_3(FeGa)_5O_{12}$ film with $Q = 58$ and a static saturation field $H_s = 42$ Oe, the jump in magnetization was found to occur in fields with $H_K = 18, -8, -18$, and -44 Oe, respectively. Clearly, in the last case, a magnetization-reversal nucleus grows, a DS is formed, and then the DS is destroyed in a single large jump of magnetiza-

tion from $+J_s$ to $-J_s$. If we relate the field H_m to the amplitude H_0 of an ac magnetic field ($H_\sim = H_0 \sin(2\pi ft)$), it becomes obvious that the higher the amplitude H_0, the later the magnetization reversal process begins in each such film and the shorter the time that is left for the growth of domains of the reversed magnetic phase. Increasing the frequency of the ac field leads to similar results.

Let us return to the dynamic domain phase diagram in Fig. 10. At fairly moderate frequencies (1 – 2 kHz) and high amplitudes of the ac field ($H_0 > 2H_s$), radial DDSs have no time to fill the entire sample because of the hysteresis, which results in the formation of DDSs shaped as multiprong stars (region *7*) whose prongs get shorter and finally disappear as the field frequency is increased. A *dynamic single-domain state* forms in the phase diagram (region *8*). It was found that this is an extremely important state, and it determines a number of specific features of the dynamic hysteresis properties of iron garnet films (see Section 5). Here, it must be emphasized that in interpreting the radial DDS → blinking stars → dynamic single-domain state transitions one must take into account the transitions of the internal structure of the domain walls (e.g., see Ref. [86]) and the changes in the dynamic characteristics of these walls (velocity V and mobility) that occur in the course of the jump in magnetization, especially if this jump ΔJ is close to $2J_s$. At present, such data are not available. Estimates of the saturation velocity V_s for the given $(YLuBi)_3(FeGa)_5O_{12}$ film made on the basis of several well-known formulas [87] and the necessary data on the gyromagnetic ratio and the damping parameter [43] have produced very moderate values for V_s ranging from 0.5 m s^{-1} to 0.03 m s^{-1}. The question of how these values correspond to real velocities remains open, however.

The amplitude – frequency region *9* of the phase diagram 'contains' *giant dynamic domains* shaped as round spots and 'floating clouds' with comblike walls (see Fig. 9). However, a giant leading center on this film can be observed only if the temperature is raised to ~40 °C [46, 58]. The destruction of the dynamic single-domain state and the transition to giant domains as the frequency of the ac field is increased and the amplitude of the field is $H_0 \sim 120$ Oe (i.e., $H_0 \sim 2.4\,H_s$) are, presumably, associated with changes in the very mechanism of formation of the reversed magnetic phase, for example, to a transition from the mechanism of growth of a fully formed microscopic domain to the mechanism of formation of reversed domains from micromagnetic inhomogeneities in the vicinity of defects [83] or to the spin-wave mechanism related to the generation of a magnetic-moment flop wave. Although in this review we cover only the low-frequency magnetic dynamics of IG films, in the case of sudden domain formation induced by a jump in magnetization, certain effects discovered by a number of researchers (A S Logginov, V V Randoshkin, V G Kleparskiĭ and others) in their studies of processes of pulsed magnetization reversal of IG films manifest themselves. Among these effects are the formation of reversed microdomains in front of a moving domain wall and the turbulent nucleation of dynamic micromagnetic structures (see numerous references in Ref. [43]).

Region *11* of the phase diagram for the given sample (see Fig. 10) 'contains' dynamic structures such as leading and domain centers and other sources of dynamic domains with smooth walls. Their characteristic dimensions, the width of rings in leading and domain centers and the diameter of CDs, are of the same order as d_0, the domain width in the initial dynamic structure (Fig. 1a).

Thus, the phase diagram gives a fuller picture of the various states of a dynamic system of magnetic domains than its separate fragments, e.g., the region of the 'anger' state (*3*) alone. We note once more that the types of DDS specified by the phase diagram are retained as long as the pump field is operating and the field parameters and temperature remain constant. The overall features of a phase diagram are reproduced in repeated experiments, provided that the experimental conditions are strictly the same.

For different samples of iron garnet films (with different values of the characteristics such as the saturation magnetization, the uniaxial anisotropy constant, and the Q factor), the phase diagrams differ significantly (e.g., compare the phase diagram in Fig. 10 to the phase diagrams in Refs [79, 80]). The experimental data are still so scant that it is impossible to speak of firmly established laws that govern the shape of the phase diagram, of quantitative dynamical and geometric parameters of the domain phases, of the special features of the various phase transitions, including hysteresis effects, and the more so of the reasons for, and mechanisms of, the DDS transformations caused by changes in the frequency and amplitude of the ac field. We have just enough data to discuss the general features of the phase diagrams for the films studied so far. When the field amplitudes are $H_0 < 0.5 - 0.3\,H_s$ and the frequency f is low, one can observe a labyrinthine DDS which, as the frequency is raised up to 50 – 100 kHz, becomes mosaic, with blocks consisting of parallel stripe domains. The boundaries of the blocks constitute a set of magnetic domain dislocations [61]. Block mobility increases with frequency, and, for certain combinations of H_0 and f, sinusoidal distortions appear at the walls of the dynamic stripe domains, so that the pattern that finally emerges is that of traveling waves [80]. Presumably, the block stripe DDS (region *1* in Fig. 10) may be assumed to be the main initial state of a multidomain sample in the 10 – 150-kHz range, and so it is the transition of this state that one should study as the amplitude of the ac field is increased.

When the field amplitude H_0 is higher than H_s and the field frequency is in the 30 – 100-kHz range, a DDS in the form of more or less ordered lattices of CDs is observed. For different samples and in different sections of the phase diagram, these lattices may be of different types: e.g., lattices of unipolar CDs or mixed lattices containing clusters of heteropolar CDs (as in Figs 7a – 7c); lattices consisting of cylindrical domains (CDs) with diameters of order d_0 and of large, even giant CDs with comblike walls; and lattices consisting of mobile CDs and practically immobile CDs. Such lattices may either surround ordered structures of leading-center type (see Fig. 7) or occupy almost the entire area of the sample [80]. Such diversity, most likely, arises from the significant differences in the dynamic characteristics of iron garnet films. There are several reasons why there may occur transitions initiated by increases in the amplitude H_0 and the frequency f from a block stripe DDS to systems that in the first approximation appear to be lattices of cylindrical domains:

(1) the excess of domain-wall velocities over the saturation velocity, the change of the walls' motion from stationary to nonstationary, and the complicated transformation of the internal structure of the domain walls and the emergence of Bloch lines, which promote destruction of stripe domains; and

(2) the time lag of changes in the position of the domain walls behind the changes in the strength of the magnetic field inside the film and, as a result, the retention of a large number of magnetization-reversal nuclei (reversed magnetic domains), which, as the field strength is lowered, grow and form a lattice of CDs.

When analyzing the observed diversity of dynamic lattices of CDs and their transformations initiated by changes in the parameters of the ac field, one must take into account the special features of the static and dynamic properties of lattices of CDs that have been thoroughly discussed by Bar'yakhtar and Gorobets in their monograph [44].

The larger part of the phase diagram (see Fig. 10 and also Refs [79, 80]) is occupied by regions of disordered DDSs called *visual chaos* and *gray background* (regions *2* and *4* in Fig. 10). In the first case, one observes violently moving (flashing) irregularly shaped domains, while in the second case, the displacement of domains is not visible and only a gray background can be observed. In the photographs and frames of video-microfilming corresponding to $f \sim 0.2-10$ kHz and $H_0 \sim 0.5-1.5\,H_s$, one can observe a disordered DDS in regions *2* and *4* consisting of arched short or more or less extended stripe domains, honeycomb-shaped single-turn spirals, ring domains, etc. A spatial–temporal dynamic (domain) chaos of this type surrounds multiturn spiral domains in the 'anger' state of the sample (see Figs 3 and 5c). Employing the terminology of Ref. [55], we might describe a disordered DDS of this type as *spiral domain chaos*.

At frequencies higher than 50–100 kHz, the disordered DDS is of a different form. This becomes quite obvious if we compare the surroundings of the dynamic SDs in Fig. 3 with the surroundings of structures of the leading-center type in Figs 7 and 8c. At moderate values of the amplitude of the ac field (e.g., see region *10* in Fig. 10), the presence of a two-phase state is quite evident. A characteristic feature of such a state is the coexistence of stripe domains and dynamic CDs. At higher values of the ac-field amplitude ($H_0 > H_s$), the main components of a disordered DDS are the heteropolar islands (clusters), consisting of CDs of different dimensions and shapes. Here, the CDs are formed in the process of destruction of stripe domains, outer rings of leading centers, emission of bubbles, etc. Presumably, the formation of a chaotic (or disordered) DDS is assisted by the theoretically predicted effects of the chaotic dynamics of a plane domain wall in the case where the velocity of this wall exceeds the saturation velocity [88, 89] and of the chaotic dynamics of a system of 180° walls in the model of plane-parallel domains [90].

Thus, a dynamic domain phase diagram provides a more complete picture of the states of a dynamic system of magnetic domains in the iron garnet films under investigation than any of its separate parts. Theoretical and experimental studies of the phase diagram that use high-speed photography and video-microfilming and computer technology to process the enormous amount of information will have to be conducted in the future.

8. Dynamic hysteresis properties of iron garnet films

The above suggests that the various features of the behavior of dynamic systems of magnetic domains in iron garnet films described in this review lead to special dynamic hysteresis properties of such films. Indeed, the following effects were detected and reported in Refs [91–93]:

(1) a '*blinking*' *hysteresis loop* in the 'anger' state of iron garnet films;

(2) *triangular hysteresis loops* in highly anisotropic films with a Q factor no smaller than 20;

(3) collapse of a triangular hysteresis loop along the vertical (magnetization) axis and transition to the *dynamic single-domain state*;

(4) stable and unstable hysteresis cycles (the effect of *chaotization of hysteresis loops*).

A specially designed experimental facility has made it possible to virtually instantaneously (with time intervals shorter than 1 s) observe DDSs and photograph the image on the oscilloscope screen of the magnetooptic hysteresis loop covering almost the entire sample (the diameter of the illuminated spot was about 3 mm). Figure 11 shows some of the results of an experiment involving the sample whose dynamic domain structures and phase diagram are depicted in Figs 3 and 10, respectively.

Experiments have shown that beyond the amplitude–frequency region of the 'anger' state in films with moderate values of the Q factor (less than 20), the dynamic hysteresis loops are of the ordinary form (Figs 11a, 11c, and 11d), while the dependences of the shape and area of the hysteresis loops on the amplitude and frequency of the ac field are the same as those described and discussed in Ref. [11]. The image of the loops on the oscilloscope screen is sharp and stable in time. In contrast, when samples in which the 'anger' state is observed in the proper amplitude–frequency region (Fig. 3f) are involved, the loop opening at the tips of the hysteresis loops suddenly changes from time to time. These loop

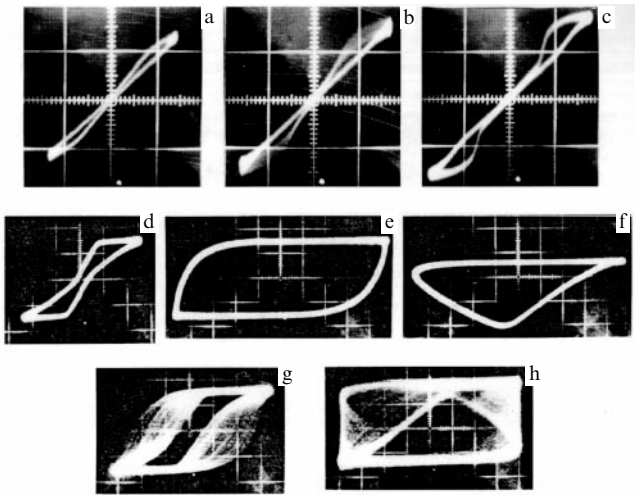

Figure 11. Dynamic hysteresis loops of the iron garnet film whose phase diagram is shown in Fig. 10, in a field $H_\sim = H_0 \sin(2\pi ft)$ with the following values of f and H_0:

	a	b	c	d	e	f	g	h
f, kHz	2	2	2	0.8	0.8	1.6	0.8	1.6
H_0, Oe	37	41	47	61	119	119	81	104

One division on the horizontal scale of the oscilloscope's graticule corresponds to 25.5 Oe. On the vertical scale, the variation of magnetization in arbitrary unit is given.

sections continuously pulsate, or blink. In the time that a photograph is taken (about 2 s), the sections may blink many times, so that the tips of the hysteresis loops appear smeared (Fig. 11b). It has been found that when many spiral domains appear or even one large multiturn SD appears, the loop opening at the tips of the hysteresis loops diminishes. Quasi-periodic appearance $\Leftrightarrow$ disappearance of spiral domains with a frequency of 0.1 – 10 Hz causes the hysteresis loops to narrow $\Leftrightarrow$ broaden with the same frequency. The 'blinking' of the tips of the hysteresis loops in the AS region corresponds to a dip in the dynamic magnetization curve [46, 91] and a decrease in the loop area, which means a reduction in the magnetization-reversal energy losses by a factor of two to three [91]. We believe that this last feature merits special attention. The self-organization of the entire ensemble of coupled (or interacting) magnetic domains in the sample manifests itself most vividly in the 'anger' state. And since in the iron garnet films that we studied self-organization causes a reduction in the magnetization-reversal energy losses, it is natural to assume that such phenomena may also occur in other materials, such as soft magnetic materials used in electrical engineering.

When highly anisotropic IG films (with $Q > 20$) are involved, as the field amplitude is raised to values exceeding the value of the static saturation field ($H_0 > H_s$), the hysteresis loop broadens, becomes a rectangular loop (Fig. 11e), and finally turns into a very strangely shaped (triangular) loop (Fig. 11f). Direct observation of DDSs and the photographing of these structures in the stroboscopic mode [92] have shown that in the case of a triangular hysteresis loop the sample does not undergo total reversal of magnetization as the field changes from $+H_0$ to $-H_0$. This type of structure belongs to region *7* of the phase diagram (see Fig. 10), i.e., consists of stars whose prongs are long. As the frequency f increases, the prongs become shorter, and the sample passes into the single-domain state (region *8* in Fig. 10). Accordingly, the hysteresis loop (Fig. 11f) becomes more constricted along the magnetization axis (the vertical axis) and finally collapses. The sample ceases to react to an external ac magnetic field.

We believe that the main reason for magnetic hysteresis is the time lag in the formation and growth of the magnetization-reversal nuclei. Filippov and Lebedev [85] developed a comprehensive theory of magnetic hysteresis in a static field related to this reason. To our knowledge, however, the behavior of the magnetization-reversal nuclei in highly anisotropic magnetic materials placed in an ac field has never been examined theoretically.

Let us now turn to a very interesting law discovered through experiments. The images of the hysteresis loops on the screen of the oscilloscope in Figs 11a, c, d, e, and f are sharp. This means that in each of these loops hundreds and thousands of magnetization-reversal cycles follow the same way during the exposition time $\tau = 2$ s. It is only natural to call such hysteresis loops *stable*, or *dynamically equilibrium*, loops.

When observing the transformations of magnetooptic hysteresis loops from constricted (Fig. 11d) to rectangular (Fig. 11e) to triangular (Fig. 11f), we passed the given intervals of the values of H_0 and f in fairly large steps. A more thorough study revealed the presence of an unexpected effect, the *chaotization of hysteresis cycles* [93]. The essence of this effect is that within narrow intervals of the values of H_0 and f, the image of hysteresis loops becomes 'smeared', or diffuse (Fig. 11g), and there is an entire spectrum of faintly outlined hysteresis loops along which, obviously, magnetization reversal rarely proceeds. It is natural to call such hysteresis cycles *unstable*, or *dynamically nonequilibrium*, loops. The coercive force H_c in these cycles may differ severalfold. Photometric measurements of such hysteresis loops have shown that, as the field amplitude increases (at $f = \text{const}$), the H_c distribution becomes sharper and sharper. What has also been established is that the scarcely distinguishable hysteresis loops appearing infrequently as fluctuations and having the highest possible value of H_c for a given field amplitude H_0 (and $f = \text{const}$) become predominant as H_0 increases. And in this way step by step we pass to the image of the hysteresis loop in Fig. 11e. This is a demonstration of a general principle: a new state is born within the old one as a result of fluctuations whose frequency gradually increases [94].

At frequencies and amplitudes of the ac field that are higher than those corresponding to Fig. 11g (see table in the caption to Fig. 11), a new feature appears in the diffuse pattern of hysteresis loops: the electron beam shows triangular hysteresis loops with the obtuse tip randomly directed up or down along the vertical axis. This produces an entire spectrum of triangular hysteresis loops (Fig. 11h), which can be called *dynamically unstable*, *nonequilibrium* hysteresis cycles. But as the field amplitude increases, a stable triangular hysteresis loop (Fig. 11f) emerges once more.

It is difficult to provide a definite answer to the question of why variations in H_0 and f lead to stable $\Leftrightarrow$ unstable $\Leftrightarrow$ stable hysteresis-loop transitions (Fig. 11, the d $\Leftrightarrow$ g $\Leftrightarrow$ e and d $\Leftrightarrow$ g $\Leftrightarrow$ h $\Leftrightarrow$ f transitions; for more details, see Ref. [93]). In this connection, Solov'ev and Filippov's results [90] are worth mentioning. These researchers theoretically analyzed the behavior of a system of plane-parallel domains in films with perpendicular anisotropy placed in a sinusoidal ac field. They found that for certain combinations of parameters of the pump field, the vibrations of the domain walls become chaotic. We cannot rule out the possibility that in our case, too, for certain combinations of H_0 and f, the boundaries of the magnetization-reversal nuclei become displaced in a random manner, which in turn initiates large disordered jumps in magnetization, i.e., leads to chaotization of the hysteresis loops. Earlier, the possibility of chaotic behavior of domain walls in an iron garnet film placed in an ac magnetic field or in the case where domain walls move in the saturation-velocity regime was pointed out in the theoretical works of Zvezdin et al. [88] and Kotova and Chetverikov [89].

To conclude this section, note that magnetization jumps, including big Barkhausen jumps, in soft magnetic materials have intensely been studied in connection with the problem of magnetic noise [95]. Interesting regularities in the nature of fluctuations of the parameters of big jumps in magnetization have been discovered (e.g., see Ref. [96]). However, we emphasize that, to our knowledge, transformations of the hysteresis loops initiated by variations in the amplitude and frequency of the ac field, demonstrated in Fig. 11 and accompanied by changes in the dynamic domain structure (see Fig. 10), have never before been observed. The theory of the anomalous dynamic hysteresis properties of highly anisotropic films with perpendicular anisotropy described in the current section must be developed with allowance for the features of DDSs discussed in the previous sections.

9. Parameters of iron garnet films with ordered dynamic domain structures

The study of a large number of iron garnet films with a single-type initial domain structure (Fig. 1a) has shown that not in all films can an 'anger' state be generated and, respectively, can dynamic SDs in DDSs of the leading-center type be formed. With a view to find the specific features in the properties of IG films with or without the 'anger' state and an ordered DDS at room temperature, we selected 21 film samples with thicknesses ranging from 1.5 to 40 μm, with DS periods $P_0 = 2d_0$ ranging from 4 to 41 μm, with a labyrinthine DS that is isotropic in the film plane (Fig. 1a), and with a coercive force H_c weaker than 1.5 Oe. For all samples placed in a dc magnetic field that was perpendicular to the film surface, i.e., was oriented along the EA, we observed the domain structure, determined the field H_{coll} of magnetic-bubble collapse, and measured the magnetooptic magnetization curves, the hysteresis loops, and used these curves to determine H_c and the static saturation field H_s (the values of H_s and H_{coll} were practically equal or differed only a little).

Measurements in a magnetic field directed parallel to the film plane and, therefore, perpendicular to the EA were used to find the anisotropy field H_a. Through the use of well-known methods (described in detail in Ref. [46]), we found the saturation magnetization J_s, the constant K of induced uniaxial magnetic anisotropy, the Q factor of the magnetic material $Q = K/(2\pi J_s^2)$, the characteristic length $l^* = \gamma/(4\pi J_s^2)$, the exchange interaction parameter A, and the wall-energy density γ. Thus, the films investigated were fully certified by the static characteristics [46].

All samples exhibited a dynamic domain structure in an ac sinusoidal magnetic field or in a field of the meander type (see Section 2) with frequencies ranging from 0.1 to 10 kHz and amplitudes up to 200 Oe. The samples in which an ordered DDS was observed and in which we were able to generate an 'anger' state were classified as group 1 samples (11 samples), while all the other samples were classified as group 2. It was found that these groups did not differ in the values of the parameters enumerated in the previous paragraph. At the same time, the dependence of the reduced period P_0/l^* of the initial labyrinthine DS on the reduced film thickness L/l^* (the curve virtually coincides with the theoretical curve of Malek and Kambersky [99]) clearly shows that the points corresponding to group 1 samples cluster around the minimum of this curve and that the values of P_0/l^* and L/l^* do not exceed 15 and 7, respectively. For group 2 samples, the values of P_0/l^* and L/l^* were higher. Apparently, at large values of L, the possible distortions of the shape of the stripe domains and their walls (e.g., the walls become corrugated near the surface) and the emerging flexural vibrations of the stripe domains [49, 100] hinder the formation of dynamic SDs or CRD systems from these domains.

Possibly, the proper relationships between the geometric parameters of the domain structure and samples should be considered as necessary but far from sufficient condition for the realization of the 'anger' state. The dynamic characteristics of the films (wall mobility, the damping coefficient, etc.) may prove to be much more important, especially when we are studying the shape of the field $H(t)$ that generates the 'anger' state, the natural frequencies of the vibrational processes in the 'anger' state of a dynamic system of magnetic domains, and the specific shape of an ordered DDS. Finding and analyzing these characteristics should be the goal of future investigations.

10. Dynamic self-organization of an ensemble of magnetic domains in amorphous films with perpendicular anisotropy

Above, we described a whole new range of effects and regularities that constitute the phenomenon of dynamic self-organization and the 'anger' state in iron garnet films. Finding and studying dynamic self-organization and the 'anger' state in other multidomain magnetic media was crucial for our investigations. As objects of our investigation, we chose amorphous gadolinium–cobalt (Gd_xCo_{1-x}) films, which exhibit perpendicular anisotropy. The statistic properties of the Kittel domain structure of Ga–Co films (Fig. 12b) are similar to those of the domain structure of IG films studied earlier. However, the microstructure and many other physical properties of single-crystal insulator IG films differ entirely from those of the amorphous metallic Gd-Co films.

By changing the composition of the Gd–Co system, we can produce films for which the magnetic compensation temperature T_{comp} will differ very little from room temperature. In this case, it becomes possible, by slightly varying the temperature of the sample, to change the saturation magnetization J_s, the static saturation field H_s, the coercive force H_c, and the domain-structure period in the demagnetized state $P_0 = 2d_0$ within very broad limits. This means an increase in the probability of arriving at such a combination of these parameters at which an 'anger' state and dynamic SDs appear in an ac magnetic field. It was this strategy of our experiment that led us to success [49, 101].

For example, in a 0.4-μm-thick $Gd_{22}Co_{78}$ film with a magnetic compensation temperature $T_{comp} = 55\,^{\circ}C$, we observed the formation of an 'anger' state and dynamic SDs on both sides of T_{comp} (almost symmetrically) in the temperature ranges from 1 to 15 °C and from 100 to 113 °C with the sample placed in an ac magnetic field $H_{\sim} = H_0 \sin(2\pi ft)$ (Figs 12a–12c). The amplitude–frequency region (H_0–f) changes with T. At $T = 100\,^{\circ}C$ (Fig. 12d), this region extends from 10 to 50 kHz in f and from 100 to 280 Oe in H_0, i.e., as compared to IG films (Figs 2c and 3f), the region is shifted to higher frequencies and amplitudes. For instance, for an IG film, the minimum frequency f_b, which limits the AS region from the left, is lower than 1 kHz, while for a Gd–Co film (Fig. 12d) this frequency is higher than 10 kHz. A possible explanation is that the coercive force of amorphous films is ten times greater than the H_c of IG films. There are also other differences between the 'anger' state and dynamic SDs of these two types of film. For example, the SDs that form in amorphous films have three or four turns at most, while the number of turns in the SDs that form in IG films may be greater than 15 (e.g., cf. Fig. 12c and Figs 3e and 4). More than that, in the 'anger' state of IG films, the multiturn SDs move quite freely in the sample, while in amorphous films, the large SDs are localized in regions where they were generated. Possibly, such behavior of the 'anger' state in amorphous films is related to their higher coercive force.

Anyway, the significance of Refs [49, 101] is that there we were able to demonstrate the phenomenon of self-organization of a dynamic ensemble of magnetic domains and the formation of spiral structures in films whose nature differs from that of iron garnet films. Hence, there is reason to believe

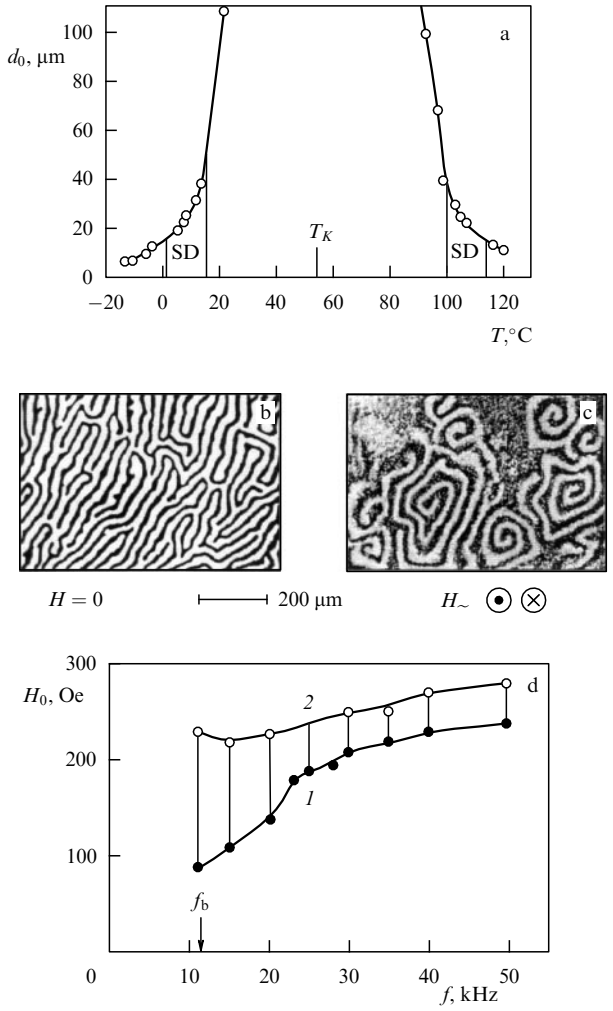

Figure 12. Temperature dependence of the stripe-domain width (a), domain structure in the demagnetized state (c) and in an alternating field $H_\sim = H_0 \sin(2\pi ft)$ with $f = 30$ kHz and $H_0 = 180$ Oe (c), and the region ($H_0 - f$) of existence of the anger state and dynamic SDs at 100 °C (d) of an amorphous gadolinium – cobalt film.

that the phenomenon of dynamic self-organization and the 'anger' state of multidomain magnetic media is universal.

11. Conclusion

Summarizing our results, we note the following:

(1) In the process of our experimental investigations, we discovered and studied the phenomenon of dynamic self-organization and the 'anger' state of a multidomain magnetic medium. Studying thin iron garnet films with perpendicular anisotropy, we found that, within a certain limited range of the amplitudes and frequencies of a low-frequency ac magnetic field that is spatially uniform and operates continuously, in the chaotically moving ensemble of magnetic domains there form, as a result of self-organization, ordered and stable dynamic domain structures (DDSs) of various types (ring, spiral, etc.). Most thoroughly studied are the dynamic spiral domains (SDs) in the frequency range from 10^2 to 10^4 Hz. It has been noted that in different films spiral domains differ in geometry and properties. We also determined the dependence of the quantitative characteristics of these DDSs on the frequency and amplitude of the ac field.

(2) It has been established that in the excited ('anger') state of a dynamic system of interacting domains, in addition to self-organization, there is self-generation of quasi-periodic processes, and that the basic quasi-periodic process here is the appearance ⇔ disappearance of ordered DDSs. The frequency of this process is several orders of magnitude lower than the field frequency and strongly depends on the characteristics of the ac field. Video-microfilming has been used to study the evolution of spiral domains in the course of their life. Quantitative characteristics of the 'anger' state such as the formation time, the lifetime, the destruction time, and the wait time for spiral domains have been introduced. Finally, the dependence of the AS parameters of the frequency and amplitude of the ac field has been established.

(3) The effect of a dc magnetic bias field on a DDS has been investigated. It has been found that weak bias fields destroy the 'anger' state, while stronger fields, comparable to or exceeding the amplitude of the ac field, may initiate new 'anger' states (called *induced* '*anger*' *states*) in such amplitude – frequency regions where no 'anger' state previously existed, or even in films where no 'anger' state was ever observed. Thus, one must consider the bias field, in addition to the frequency and amplitude of the ac field, as the third effective parameter controlling the state of a dynamic ensemble of magnetic domains. This suggests that three-dimensional AS diagrams should be built.

(4) In the region of higher frequencies ($10^4 - 10^5$ Hz), DDSs with an extremely wide range of geometric and other properties have been detected, namely, structures of the leading-center type that periodically emit concentric ring magnetic domains, 'blinking stars,' sources of large bubbles containing CDs, giant structures with comblike walls, rotating vortices, etc. It has been established that changes in the frequency and amplitude of the ac magnetic field may initiate a transformation of a single source of dynamic domains related to a local defect. This suggested the idea of a *complete dynamic domain phase diagram* in the amplitude – frequency plane. The different regions in the diagram correspond to different types of ordered or disordered dynamic structures that clearly differ in their configuration and dynamic behavior, i.e., dynamic domain phases. Such diagrams have been built and studied for several films, and some general regularities in the arrangement of the amplitude – frequency regions for single-type DDSs in the diagrams of different samples have been established. These results make it possible to repeatedly reproduce a specific DDS type in a particular sample. More than that, further studies of dynamic domain phase diagrams and the gathering and systematization of experimental data will make it possible to predict the dynamic behavior of the domain structure of any iron garnet film (and, possibly, of any thin film with perpendicular anisotropy) with known magnetic constants and thickness.

(5) The dynamic hysteresis properties of iron garnet films have been studied in the audiofrequency range ($10^2 - 10^4$ Hz). The effect of hysteresis-loop blinking has been detected in the AS region. It amounts to rapid quasi-periodic decrease ⇔ increase of the loop area, which in turn is related to the appearance ⇔ disappearance of spiral domains. It has been established that for highly anisotropic films with a well-defined limited region of amplitudes and frequencies, the sample ceases to react to the ac field and remains magnetized almost to the saturation level, i.e., the single-domain state sets in. It has also been found that, as the frequency and amplitude of the field increase and the single-domain state is

approached, the hysteresis loop is distorted, first becoming rectangular and then triangular. Complete correspondence between such hysteresis loops and changes in the DDS in an oscillating magnetic field has been established. Within a narrow interval of amplitudes and frequencies of the ac field, partial or complete chaotization of the hysteresis cycles has been discovered.

(6) Today, there is no theory capable of substantiating and quantitatively describing, on the basis of a unique approach, the entire set of new effects and regularities that constitute the phenomenon of dynamic self-organization and the 'anger' state of a multidomain magnetic medium. However, the publications discussed in this review, especially those written in recent years (Refs [73, 75, 76, 102–104]), show that the search for the ways of building such a theory is extremely active, e.g., solutions to micromagnetic equations corresponding to spiral and ring dynamic structures have been found and the dynamic stability of large systems of concentric ring domains has been justified.

(7) The existence of self-organization, i.e., disordered $\Leftrightarrow$ ordered DDS transitions in a dynamic domain ensemble in whose evolution one can clearly observe periodic (quasi-periodic) processes (formation $\Leftrightarrow$ destruction of ring and spiral domains, the emission of domains by local sources of the leading-center type, etc.), points to the excitability of a multidomain magnetic medium, to its activity. This makes it possible to classify such media as objects of synergetics. In some respects, the geometry of ordered DDSs and their behavior are, at first glance, strikingly similar to the autowave structures quite thoroughly studied in synergetics, e.g., to spiral and concentric ring autowaves in diffusion-active media. However, spiral and concentric ring dynamic domains that form in the 'anger' state of films with perpendicular anisotropy differ significantly from autowaves both in the conditions of excitation (the films are in a constantly operating ac field) and in the established set of properties. Hence, multidomain magnetic media should be classified as new objects of synergetics, and there are no well-established theoretical models for describing dynamical phenomena in such objects.

Acknowledgements. I am grateful to V L Ivashintseva, V P Klin, V A Matveev, V I Chani, and A Ya Chervonenkis for supplying iron garnet films in ample quantities. My sincere thanks are to M S Rebrin and A A Rusinov for the help they provided in preparing this review for press. This work was supported in part by the Fundamental Research in Natural Sciences program (Grant E00-3.4-258), the CRDF program (Grant REC-005), and the Universities of Russia program (Grant 01.015.99).

References

1. Zaĭkova V A, Startseva I E, Filippov B N *Domennaya Struktura i Magnitnye Svoĭstva Elektrotekhnicheskikh Staleĭ* (Domain Structure and Magnetic Properties of Electric Steel) (Moscow: Nauka, 1992)
2. Malozemoff A P, Slonczewski J C *Magnetic Domain Walls in Bubble Materials* (New York: Academic Press, 1979) [Translated into Russian (Moscow: Mir, 1982)]
3. Randoshkin V V, Chervonenkis A Ya *Prikladnaya Magnitooptika* (Applied Magnetooptics) (Moscow: Energoatomizdat, 1990)
4. Kandaurova G S, Sviderskiĭ A É *Pis'ma Zh. Eksp. Teor. Fiz.* **47** 410 (1988) [*JETP Lett.* **47** 490 (1988)]
5. Kandaurova G S, Sviderskiĭ A É *Pis'ma Zh. Tekh. Fiz.* **14** 777 (1988) [*Sov. Tech. Phys. Lett.* **14** 346 (1988)]
6. Kandaurova G S *Dokl. Akad. Nauk SSSR* **308** 1364 (1989) [*Sov. Phys. Dokl.* **34** 918 (1989)]
7. Kandaurova G S, Chervonenkis A Ya, Sviderskiĭ A É *Fiz. Tverd. Tela* (Leningrad) **31** (6) 238 (1989) [*Sov. Phys. Solid State* **31** 1049 (1989)]
8. Kandaurova G S, Sviderskiĭ A É *Zh. Eksp. Teor. Fiz.* **97** 1218 (1990) [*Sov. Phys. JETP* **70** 684 (1990)]
9. Loskutov A Yu, Mikhaĭlov A S *Vvedenie v Sinergetiku* (Foundations of Synergetics) (Moscow: Nauka, 1990) [Translated into English (Berlin: Springer, 1990)]
10. Borisov A B, Feĭgin V A, Filippov B N *Fiz. Tverd. Tela* (Leningrad) **33** 2316 (1991) [*Sov. Phys. Solid State* **33** 1304 (1991)]
11. Dikshteĭn I E et al. *Zh. Eksp. Teor. Fiz.* **100** 1606 (1991) [*Sov. Phys. JETP* **73** 888 (1991)]
12. Lisovskiĭ F V et al. *Zh. Eksp. Teor. Fiz.* **103** 213 (1993) [*JETP* **76** 116 (1993)]
13. Gobov Yu L, Shmatov G A *Fiz. Met. Metalloved.* **78** (1) 39 (1994) [*Phys. Met. Metallogr.* **78** 26 (1994)]
14. Lisovskiĭ F V, Mansvetova E G, Pak Ch M *Zh. Eksp. Teor. Fiz.* **108** 1031 (1995) [*JETP* **81** 567 (1995)]
15. Borisov A B, Yalyshev Yu I *Fiz. Met. Metalloved.* **79** (5) 18 (1995) [*Phys. Met. Metallogr.* **79** 482 (1995)]
16. Lamonova K V, Mamaluĭ Yu A, Siryuk Yu A *Fiz. Tekh. Vys. Davl.* **6** (1) 33 (1996)
17. Zablotskiĭ V A, Mamaluĭ Yu A, Soĭka E N *Fiz. Tekh. Vys. Davl.* **7** (2) 74 (1997)
18. Lamonova K V, Mamaluĭ Yu A *Fiz. Tekh. Vys. Davl.* **7** (2) 82 (1997)
19. Mamaluĭ Yu A, Soĭka E N *Fiz. Tekh. Vys. Davl.* **9** (4) 88 (1999)
20. Shagalov A G *Fiz. Met. Metalloved.* **84** (5) 24 (1997) [*Phys. Met. Metallogr.* **84** 466 (1997)]
21. Kooy C, Enz U *Philips Res. Rep.* **15** (1) 7 (1960)
22. Logunov M V, Moiseev N V, in *Novye Magnitnye Materialy Mikroelektroniki: Tez. Dokl. XV Vseros. Shkoly-Seminara, 18–21 Iyunya 1996, Moskva* (New Magnetic Materials of Microelectronics: Abstracts of Reports at the 15th Nat. Workshop, June 18–21, 1996, Moscow, Russia) (Moscow: URSS, 1996) p. 427
23. Moiseev N V, Author's Abstract of Thesis for Candidate of Phys.-Math. Sci. (Moscow: Moscow State Univ., 1998)
24. Lamonova K V, Mamalui Yu A, Siryuk Yu A *Fiz. Tekh. Vys. Davl.* **6** (4) 49 (1996)
25. Kandaurova G S, Ivanov Yu V *Fiz. Met. Metalloved.* **76** (1) 49 (1993) [*Phys. Met. Metallogr.* **76** 31 (1993)]
26. Ignatchenko V A et al., Preprint No. 479 (Krasnoyarsk: Institute of Physics of the Siberian Division of the USSR Academy of Sciences, 1988)
27. Ignatchenko V A et al. *Zh. Eksp. Teor. Fiz.* **98** 593 (1990) [*Sov. Phys. JETP* **71** 331 (1990)]
28. Vlasko-Vlasov V K et al. *Fiz. Tverd. Tela* (Leningrad) **24** 1255 (1982)
29. Dragoshanskiĭ Yu N *Fiz. Met. Metalloved.* **77** (1) 95, 106 (1994) [*Phys. Met. Metallogr.* **77** 53, 61 (1994)]
30. Kandaurova G S *Izv. Vyssh. Uchebn. Zaved. Fiz.* (8) 148 (1971)
31. Chetkin M V, Akhutkina A I, Shapaeva T B *Mikroelektronika* **27** 370 (1998) [*Russ. Microelectron.* **27** 342 (1998)]
32. Soĭka E N, Author's Abstract of Thesis for Candidate of Phys.-Math. Sci. (Donetsk: Donetsk State Univ., 1998)
33. Soĭka E N *Fiz. Tekh. Vys. Davl.* **8** (3) 65 (1998)
34. Shur Ya S, Glazer A A, Gass V G *Fiz. Tverd. Tela* (Leningrad) **17** 976 (1975)
35. Solov'ev M M, Onoprienko L G *Fiz. Met. Metalloved.* **48** 774 (1979)
36. Hanna S M et al. *IEEE Trans. Magn.* **MAG-19** 1802 (1983)
37. Logunov M V, Randoshkin V V, in *XVIII Vsesoyuz. Konf. po Fizike Magnitnykh Yavleniĭ, Kalinin, 1988* (Proc. 18th All-Union Conf. on Physics of Magnetic Phenomena, Kalinin, Russia, 1988) Pt. 1 (Kalinin: Izd. KGU, 1988) p. 235
38. Logunov M V, Randoshkin V V, Inventors' Certificate No. 1675950 (Priority as of July 7, 1989)
39. Mamalui Y A, Lamonova K V, Soika E N *J. Phys. IV* (Paris) **8** Pr2-393 (1998)
40. Ges' A P et al. *Pis'ma Zh. Eksp. Teor. Fiz.* **52** 1079 (1990) [*JETP Lett.* **52** 476 (1990)]
41. Fedotova V V, Ges' A P, Gorbachevskaya T A *Fiz. Tverd. Tela* (S.-Peterburg) **37** 2835 (1995) [*Phys. Solid State* **37** 1563 (1995)]
42. Siryuk Yu A, Smirnov V V *Fiz. Tekh. Vys. Davl.* **9** (3) 102 (1999)

43. Randoshkin V V *Tr. Inst. Obshch. Fiz. Ross. Acad. Nauk* **35** 49 (1992)
44. Bar'yakhtar V G, Gorobets Yu I *Tsilindricheskie Magnitnye Domeny i Ikh Reshetki* (Magnetic Bubbles and Their Lattices) (Kiev: Naukova Dumka, 1988)
45. Lisovskiĭ F V, Mansvetova E G *Fiz. Tverd. Tela* (Leningrad) **31** (5) 273 (1989) [*Sov. Phys. Solid State* **31** 876 (1989)]
46. Sviderskiĭ A E, Thesis for Candidate of Phys.-Math. Sci. (Ekaterinburg: Ural State Univ., 1994)
47. Kim P D, Poluyan E S, Kvan Do Chen, in *Novye Magnitnye Materialy Mikroelektroniki: Tez. Dokl. XII Vsesoyuz. Shkoly-Seminara, 30 Sent.–6 Okt. 1990, Novgorod* (New Magnetic Materials of Microelectronics: Abstracts of Reports at the 12th All-Union Workshop, Sept. 30–Oct. 6, 1990, Novgorod, Russia) Pt. 2 (Novgorod: Novgorodoblmashinform, 1990) p. 182
48. Nikolaev A V, Onishchuk V N, Logginov A S, in *Novye Magnitnye Materialy Mikroelektroniki: Tez. Dokl. XV Vseros. Shkoly-Seminara, 18–21 Iyunya 1996, Moskva* (New Magnetic Materials of Microelectronics: Abstracts of Reports at the 15th Nat. Workshop, June 18–21, 1996, Moscow, Russia) (Moscow: URSS, 1996) p. 398
49. Ivanov V E, Kandaurova G S *Fiz. Met. Metalloved.* **87** (6) 57 (1999) [*Phys. Met. Metallogr.* **87** 516 (1999)]
50. Loginov I A, Logunov M V, Randoshkin V V *Zh. Tekh. Fiz.* **60** (9) 121 (1990) [*Sov. Phys. Tech. Phys.* **35** 1076 (1990)]
51. Kandaurova G S et al. *Pis'ma Zh. Eksp. Teor. Fiz.* **63** 453 (1996) [*JETP Lett.* **63** 478 (1996)]
52. Kandaurova G S, Rusinov A A *Pis'ma Zh. Eksp. Teor. Fiz.* **65** 60 (1997) [*JETP Lett.* **65** 63 (1997)]
53. Kandaurova G S, Rusinov A A *Fiz. Tverd. Tela* (S.-Peterburg) **40** 1865 (1998) [*Phys. Solid State* **40** 1691 (1998)]
54. Vasil'ev V A, Romanovskiĭ Yu M, Yakhno V G *Avtovolnovye Protsessy* (Autowave Processes) (Ed. D S Chernavskiĭ) (Moscow: Nauka, 1987)
55. Rabinovich M I, Ezersky A B *Dinamicheskaya Teoriya Formoobrazovaniya* (The Dynamics of Patterns) (Moscow: Yanus-K, 1998) [Translated into English (Singapore: World Scientific, 2000)]
56. Vlasko-Vlasov V K, Dedukh L M, Nikitenko V I, Preprint (Chernogolovka: Institute of Solid State Physics of the USSR Academy of Sciences, 1981)
57. Nikolaev V V, in *Teoriya i Modelirovanie na EVM Defektnykh Struktur v Kristallakh* (Theory and Computer Simulation of Defect Structures in Crystals) (Eds A N Orlov, B A Grinberg) (Sverdlovsk: Izd. UNTs AN SSSR, 1986) p. 117
58. Kandaurova G S, Sviderskiĭ A É, in *Statisticheskie i Dinamicheskie Svoĭstva Magnitouporyadochennykh Kristallov* (Static and Dynamic Properties of Magnetically Ordered Crystals) (Eds M M Farztdinov et al.) (Ufa: Izd. BashGU, 1990) p. 8
59. Kandaurova G S, Sviderskiy A E *Physica B* **176** 213 (1992)
60. Kandaurova G S *Dokl. Ross. Akad. Nauk* **331** 428 (1993) [*Phys. Dokl.* **38** 342 (1993)]
61. Palatnik L S, Lukashenko L I *Fiz. Met. Metalloved.* **29** 782 (1970)
62. Dragoshanskiĭ Yu N, Khan E B, Zaĭkova V A *Fiz. Met. Metalloved.* **39** 289 (1975)
63. Kandaurova G S *Fiz. Met. Metalloved.* **79** (1) 158 (1995) [*Phys. Met. Metallogr.* **79** 84 (1995)]
64. Mal'tsev V N, Kandaurova G S, Rusinov A A *Phys. Met. Metallogr.* **92** (Suppl. 1) S18 (2001)
65. Mal'tsev V N, Fakhrutdinov N M *Fiz. Met. Metalloved.* **88** (1) 17 (1999) [*Phys. Met. Metallogr.* **88** 13 (1999)]
66. Dötsch H *AIP Conf. Proc.* **29** 78 (1976) (see [2], p. 352)
67. Druyvesteyn W F, DeJang F A *Philips Res. Rep.* **25** 415 (1970)
68. DeJang F A, Druyvesteyn W F, Verhulst A G H *J. Appl. Phys.* **42** 1270 (1971)
69. Antonov A V et al. *Fiz. Tverd. Tela* (Leningrad) **14** 1901 (1972)
70. Mal'tsev V N, Kandaurova G S, Fakhrutdinov N M, in *Novye Magnitnye Materialy Mikroelektroniki: Tez. Dokl. XVI Mezhd. Shkoly-Seminara, 23–26 Iyunya 1998, Moskva* (New Magnetic Materials of Microelectronics: Abstracts of Reports at the 16th Intern. Workshop, June 23–26, 1998, Moscow, Russia) Pt. 2 (Moscow: URSS, 1998) p. 600
71. Gal'tsev A F, Yalyshev Yu I *Fiz. Met. Metalloved.* **85** (4) 5 (1998) [*Phys. Met. Metallogr.* **85** 379 (1998)]
72. Gal'tsev A F, Author's abstract of Cand. Sci. (Phys.–Math.) thesis (Ekaterinburg, Ural State Railroads University, 2000)
73. Gal'tsev A F, Yalyshev Yu I *Fiz. Met. Metalloved.* **89** (3) 24 (2000) [*Phys. Met. Metallogr.* **89** 230 (2000)]
74. Maltsev V N, Kandaurova G S, in *Proc. of the First Euro-Asian Symp. "Trends in Magnetism", EASTMAG-2001, Ekaterinburg, Russia, Feb. 27 — March 2, 2001* (Ekaterinburg, 2001) p. 92
75. Mal'tsev V N, Fakhrutdinov N M *Pis'ma Zh. Eksp. Teor. Fiz.* **73** 21 (2001) [*JETP Lett.* **73** 17 (2001)]
76. Mal'tsev V N, Kandaurova G S *Phys. Met. Metallogr.* **92** (Suppl. 1) S22 (2001)
77. Kandaurova G S, Kipshakbaeva J A *Pis'ma Zh. Eksp. Teor. Fiz.* **62** 64 (1995) [*JETP Lett.* **62** 72 (1995)]
78. Kandaurova G S, Sviderskiĭ A É *Fiz. Tverd. Tela* (S.-Peterburg) **38** 1393 (1996) [*Phys. Solid State* **38** 770 (1996)]
79. Kandaurova G S, Kipshakbaeva Zh A *Fiz. Tverd. Tela* (S.-Peterburg) **37** 1058 (1995) [*Phys. Solid State* **37** 574 (1995)]
80. Kandaurova G S, Rusinov A A *Dokl. Ross. Akad. Nauk* **340** 610 (1995) [*Phys. Dokl.* **40** 53 (1995)]
81. Kandaurova G S, Shur Ya S, Deryagin A V *Izv. Akad. Nauk SSSR Ser. Fiz.* **36** 1591 (1972)
82. Kandaurova G S, Thesis for Doctorate of Phys.-Math. Sci (Sverdlovsk: Ural State University, Institute of Metal Physics, 1973)
83. Kandaurova G S, Deryagin A V, Lagutin A E *Phys. Status Solidi A* **27** 429 (1975)
84. Khrabrov V I *Fiz. Tverd. Tela* (Leningrad) **15** 148 (1973)
85. Filippov B N, Lebedev Yu G *Fiz. Met. Metalloved.* **36** 933 (1973)
86. Nikitenko V I et al. *Pis'ma Zh. Tekh. Fiz.* **8** 149 (1982)
87. Volkov V V, Bokov V A, Karpovich V I *Fiz. Tverd. Tela* (Leningrad) **24** 2328 (1982)
88. Zvezdin A K, Kulagin N E, Red'ko V G *Fiz. Met. Metalloved.* **45** 497 (1978)
89. Kotova E E, Chetverikov V M *Fiz. Tverd. Tela* (Leningrad) **32** 1269 (1990) [*Sov. Phys. Solid State* **32** 748 (1990)]
90. Solov'ev M M, Filippov B N *Fiz. Tverd. Tela* (S.-Peterburg) **39** 2036 (1997) [*Phys. Solid State* **39** 1821 (1997)]
91. Kandaurova G S, Osadchenko V Kh *Pis'ma Zh. Tekh. Fiz.* **20** (21) 24 (1994) [*Tech. Phys. Lett.* **20** 864 (1994)]
92. Kandaurova G S, Osadchenko V Kh *Pis'ma Zh. Tekh. Fiz.* **21** (20) 11 (1995) [*Tech. Phys. Lett.* **21** 819 (1995)]
93. Kandaurova G S, Osadchenko V Kh *Dokl. Ross. Akad. Nauk* **365** 181 (1999) [*Dokl. Phys.* **44** 150 (1999)]
94. Prigogine I *From Being to Becoming: Time and Complexity in the Physical Sciences* (San Francisco: W.H. Freeman, 1980) [Translated into Russian (Moscow: Nauka, 1985)]
95. Kolachevskiĭ N N *Magnitnye Shumy* (Magnetic Noise) (Moscow: Nauka, 1971)
96. Litvinenko A A, Lavrent'ev A G, Ponomarev Yu F *Fiz. Met. Metalloved.* **55** 102 (1983)
97. Kandaurova G S et al. *Pis'ma Zh. Tekh. Fiz.* **20** (16) 40 (1994) [*Tech. Phys. Lett.* **20** 663 (1994)]
98. Kandaurova G S et al. *J. Magn. Magn. Mater.* **140–144** 2135 (1995)
99. Malek Z, Kambersky V *Czech. J. Phys.* **8** 416 (1958)
100. Vaĭsman F L, Gorobets Yu I, Denisov S I *Ukr. Fiz. Zh.* **31** 234 (1986)
101. Kandaurova G S, Ivanov V E *Pis'ma Zh. Eksp. Teor. Fiz.* **66** 688 (1997) [*JETP Lett.* **66** 720 (1997)]
102. Borisov A B *Pis'ma Zh. Eksp. Teor. Fiz.* **73** 279 (2001) [*JETP Lett.* **73** 242 (2001)]
103. Gorobets Yu I, Dzhezherya Yu M, Mironenko L P *Zh. Eksp. Teor. Fiz.* **118** 189 (2000) [*JETP* **91** 167 (2000)]
104. Vedmedenko E Yu, Ghazali A, Lévy J-C S *Phys. Rev. B* **59** 3329 (1999)